Gravitational dark matter: Free streaming and phase space distribution

Md Riajul Haque* and Debaprasad Maity†
Department of Physics, Indian Institute of Technology Guwahati, Guwahati, Assam, India, 781039

(Received 9 January 2022; accepted 24 June 2022; published 12 July 2022)

Gravitational dark matter (DM) is the simplest possible scenario that has recently gained interest in the early Universe cosmology. In this scenario, DM is assumed to be produced from the scattering of inflatons through the gravitational interaction during reheating. Gravitational production from the radiation bath will be ignored as our analysis shows it to be suppressed for a wide range of reheating temperatures $(T_{\rm re})$. Ignoring any other internal parameters except the DM mass (m_Y) and spin, a particular inflation model such as α attractor, with a specific scalar spectral index (n_s) has been shown to uniquely fix the DM mass of the present Universe. For fermion type DM, we found the mass m_f should be within $(10^4\text{–}10^{13})$ GeV, and for boson/vector type DM, the mass m_s/m_X turned out to be within $(1.2\times10^{-14}/9.6\times10^{-14}\text{–}10^{13})$ GeV. Interestingly, if the inflaton equation of state $\omega_\phi \to 1/3$, the DM mass also approaches towards unique value, $m_f \sim 10^{10}$ GeV and $m_s(m_X) \sim 10^3(8\times10^3)$ GeV. We further analyzed the phase space distribution f_Y and free streaming length $\lambda_{\rm fs}$ of these gravitationally produced DM. f_Y, which is believed to encode important information about DM, contains a characteristic primary peak at the initial time where the gravitational production is maximum for both fermionic and bosonic DM. Apart from this fermionic phase space, the distribution function contains an additional peak near the inflaton and fermion mass equality $(m_Y \sim m_\phi)$ arising for $\omega_\phi > 5/9$. Furthermore, the height of this additional peak turned out to be increasing with decreasing $T_{\rm re}$ and at some point, dominates over the primary one. Since reheating is a causal process and DM is produced during this phase, gravitational instability forming small-scale DM structures during this period will encode those phase space information and be observed at present. The crucial condition of forming such a small-scale DM structure during reheating suggests that the $\lambda_{\rm fs}$ must be less than the length scale associated with the mode reentering the Hubble radius at the end of reheating $\lambda_{\rm re}$, which has been analyzed in detail. We further estimate in detail the range of scales within which the above condition will be satisfied for different masses of scalar, fermionic, and vector DM. Finally, we end by stating the fact that all our results are observed to be insensitive on the parameter α of the inflaton potential within the allowed range set by the latest Planck and BICEP/Keck results.

DOI: 10.1103/PhysRevD.106.023506

I. INTRODUCTION

Cosmological observation over more than half a century made us believe that the observable Universe is made of visible and invisible components [1–8]. Regarding the visible components, we have acquired and inculcated a great deal of knowledge about its very existence and fundamental properties. However, apart from the existential evidences through multiple observations such as galaxy rotation curve, large scale structure, and cosmic microwave background (CMB) [1,9–13], the invisible components are far from our present understanding. Gravitational dark matter (DM) is one of the invisible components that attracts lot of attention due to its seemingly unavoidable entente with the visible components in quantum field theoretic framework [14–35]. Even though very few effective field theory parameters such as the mass and cross section are sufficient to explain the very existence of DM, ignorance/nondetection [36–40] of its fundamental characters may seem indicative to suffering of going beyond the present framework of experimental and theoretical approaches [41–44]. A list of conventional particle physics approaches towards DM production being nearly exhaustive, ideas of the gravitational mechanism of DM [45–56] seem to suggest that the simplest possibilities going beyond the convention still have a lot of unexplored provisions. Gravity so far plays an extremely passive role in understanding the physical properties of standard model particles. However, difficulties in incorporating gravity in the quantum field theory framework are the fundamental reason behind

*riaju176121018@iitg.ac.in
†debu@iitg.ac.in

this. Nevertheless, based on our present understanding, the physical laws depend on the energy scale of interest. At low energy ($\lesssim$1 TeV), the SM particles may have effectively isolated themselves from gravity as long as their fundamental properties are concerned. At high energy, however, this must not be true; rather, particles and gravity may not have independent identities on their own. String theory is an elegant example that subscribes to such an idea. The gravitational production of DM may fall along this line of thought. At the classical level, Einstein's equivalence principle suggests that gravity universally couples with particles irrespective of their intrinsic properties except for mass. However, if we tend to apply this at the quantum level, where two different particle sectors are coupled through gravitons, the production cross section does depend on the intrinsic properties such as spin and charge, hence violating the equivalence principle. In this paper, we study one of such scenarios where DM is produced through inflaton annihilating into fermion/bosonic through s-channel graviton exchange. Given an inflationary model, our focus will be on the reheating phase of the Universe. Considering the reheating phase with matter domination, such a scenario has already been studied [48,49]. We generalize such a study for an arbitrary reheating equation of state. We also include the effect of production from the radiation bath for completeness. Hence, the produced DM will have thermal and nonthermal components that are generically noncold in nature. These different production mechanisms of noncold DM lead us to further study in detail their phase-space distribution and free streaming length depending upon the reheating equation of state. We will see how depending upon the type of DM, the distribution function contains distinct features and its dependence on the reheating equation of state. Those properties play a significant role in the clustering of matter on galactic and subgalactic scales [57–59]. Observing those small scale matter power spectra by mapping the Lyman-α [60–67] forest of absorption lines of light from low redshift ($z = 2$–4) quasars can differentiate different noncold DM production mechanism and their intrinsic properties.

II. BOLTZMANN FRAMEWORK

After the period of exponential expansion, the inflaton field begins to oscillate around its minima with a decaying amplitude. In the framework of quantum field theory, the time-dependent inflaton field can naturally decay into various daughter fields such as radiation, DM particles, etc. However, the decay process nontrivially depends on the inflaton coupling with those daughter fields. In order to have successful reheating, the inflaton is generically assumed to have direct coupling with the radiation field, which will be the dominating component after the end of reheating. However, due to its subdominant nature, the probability of the solely gravitational production of DM can survive in some region of parameter space, which has already been observed in [48]. In this section, we first describe the framework of such a scenario. For completeness, DM is assumed to be produced from the radiation bath with a thermal-averaged cross section $\langle\sigma v\rangle$ as a free parameter and annihilation of inflatons through gravitational interaction. However, still, there is an assumption in our DM production framework that the inflaton sector coupled with the DM sector through only gravitational interaction; therefore, we ignore any nongravitational interaction between inflaton and DM. The gravitational production of DM has been proved to be dominated by the annihilation of inflaton zero modes through the s-channel graviton exchange process; namely, $\phi\phi \to SS/ff/XX$, where ϕ is the inflaton and S, f, and X indicate scalar, fermionic, and vector DM, respectively [51–53]. The interaction Lagrangian for s-channel gravitational production of DM can be universally described by the coupling of the DM energy-momentum tensor $T^{\mu\nu}$ with the tensor metric perturbation $h_{\mu\nu}$ as [45–47]

$$\mathcal{L} = \frac{1}{2M_p}(h_{\mu\nu}T^{\mu\nu}_{\phi} + h_{\mu\nu}T^{\mu\nu}_{S/f/X}). \tag{1}$$

With this action, the associated production rate of DM can be calculated from the scattering or annihilation rate identified as [48,50]

$$\Gamma_{\phi\phi\to SS} = \frac{\rho_\phi m_\phi}{1024\pi M_p^4}\left(1+\frac{m_s^2}{2m_\phi^2}\right)^2\sqrt{1-\frac{m_s^2}{m_\phi^2}}, \tag{2}$$

$$\Gamma_{\phi\phi\to ff} = \frac{\rho_\phi m_f^2}{4096\pi M_p^4 m_\phi}\left(1-\frac{m_f^2}{m_\phi^2}\right)^{\frac{3}{2}}, \tag{3}$$

$$\Gamma_{\phi\phi\to XX} = \frac{\rho_\phi m_\phi}{32768\pi M_p^4}\sqrt{1-\frac{m_X^2}{m_\phi^2}}\left(4+4\frac{m_X^2}{m_\phi^2}+19\frac{m_X^4}{m_\phi^4}\right), \tag{4}$$

where $m_{s/f/X}$ is the mass of the scalar, fermionic, and vector DM, respectively, and the effective mass of the inflaton is symbolized as m_ϕ. At this point, we would like to point out that gravitational production of DM from radiation is also possible, and the production rate per unit time per unit volume is followed by Eq. (30). Such production is strongly suppressed compared to the production from inflaton, which we have shown in Sec. V. However, for a high reheating temperature $10^{15} \gtrsim T_{\rm re} \gtrsim 10^{13}$ GeV, fermion type DM gravitationally produced from the radiation bath has been observed to satisfy the correct abundance in a certain range of fermion mass. We have numerically checked the results (see section-V for details). We will not include this possibility in detail in our subsequent mathematical discussions. However, we will describe the numerical results of such a scenario as we go along.

We investigate the detailed dynamics of reheating by solving the following Boltzmann equations with three density components for inflaton ρ_ϕ, radiation ρ_r, and the total DM number density $n_Y = (n_Y^r + n_Y^\phi)$ as [68–70]

$$\dot{\rho}_\phi + 3H(1+\omega_\phi)\rho_\phi + (\Gamma_\phi + \Gamma_{\phi\phi\to YY})\rho_\phi(1+\omega_\phi) = 0, \tag{5}$$

$$\dot{\rho}_r + 4H\rho_r - \Gamma_\phi\rho_\phi(1+\omega_\phi) - 2\langle\sigma v\rangle\langle E_Y\rangle^r[(n_Y^r)^2 - (n_Y^{eq})^2] = 0, \tag{6}$$

$$\dot{n}_Y^r + 3Hn_Y^r + \langle\sigma v\rangle[(n_Y^r)^2 - (n_Y^{eq})^2] = 0, \tag{7}$$

$$\dot{n}_Y^\phi + 3Hn_Y^\phi - \frac{\rho_\phi(1+\omega_\phi)}{\langle E_Y\rangle^\phi}\Gamma_{\phi\phi\to YY} = 0, \tag{8}$$

where the inflaton energy density is transferred into the radiation with a constant decay width Γ_ϕ. Furthermore, n_Y^r and n_Y^ϕ are the DM number density associated with the production from the thermal bath [68] and the scattering of the inflaton field through gravitational interaction, respectively. $\langle E_Y\rangle^r = \sqrt{m_Y^2 + (3T_{\rm rad})^2}$ and $\langle E_Y\rangle^\phi = \sqrt{m_Y^2 + m_\phi^2}$ are the average energy per DM particle produced from the thermal bath [68] and the scattering of inflatons, respectively. The equilibrium number density of the DM particles can be expressed by the modified Bessel function of the second kind as

$$n_Y^{eq} = \frac{\tilde{g}_Y T_{\rm rad}^3}{2\pi^2}\left(\frac{m_Y}{T_{\rm rad}}\right)K_2\left(\frac{m_Y}{T_{\rm rad}}\right). \tag{9}$$

Additionally, the energy associated with each gravitationally produced DM particle can be calculated from the energy and momentum conservation of the annihilation-like $\phi\phi \to SS/ff/XX$ process as

$$0 = p_1 + p_2; \qquad 2m_\phi = \sqrt{p_1^2 + m_Y^2} + \sqrt{p_2^2 + m_Y^2} = 2\sqrt{p_1^2 + m_Y^2}. \tag{10}$$

Here, p_1 and p_2 are the momenta of two gravitationally produced DM particles. The above equations assume the fact that the homogeneous background inflaton is at rest, and hence, the energy stored in each gravitationally produced DM particle will be of the order of m_ϕ. In order to solve the above set of Boltzmann equations, we define the following dimensionless variables corresponding to different energy components:

$$\Phi = \frac{\rho_\phi A^{3(1+\omega_\phi)}}{(m_\phi^{\rm end})^4}, \quad R = \frac{\rho_r A^4}{(m_\phi^{\rm end})^4}, \quad Y^r = \frac{n_Y^r A^3}{(m_\phi^{\rm end})^3}, \quad Y^\phi = \frac{n_Y^\phi A^3}{(m_\phi^{\rm end})^3}, \tag{11}$$

where $A = a/a_{\rm end}$ and $m_\phi^{\rm end}$ are the normalized scalar factor and the effective mass of the inflaton field at the end of the inflation, respectively. $m_\phi^{\rm end} = \partial_\phi^2 V(\phi_{\rm end})$. This modification factor $m_\phi^{\rm end}$ increases the stability of the numerical solution. In terms of new dimensionless variables, Eqs. (5)–(8) can be written as

$$\Phi' = -c_1(\Gamma_\phi + \Gamma_{\phi\phi\to YY})\frac{A^{1/2}\Phi}{\mathbf{H}},$$
$$R' = c_1\Gamma_\phi\frac{A^{\frac{3(1-2\omega_\phi)}{2}}\Phi}{\mathbf{H}} + 2\sqrt{3}\frac{A^{-3/2}\langle\sigma v\rangle\langle E_Y\rangle^r M_p}{\mathbf{H}} \times [(Y^r)^2 - Y_{\rm eq}^2],$$
$$(Y^r)' = -\sqrt{3}\frac{A^{-5/2}\langle\sigma v\rangle M_p m_\phi^{\rm end}}{\mathbf{H}}[(Y^r)^2 - Y_{\rm eq}^2],$$
$$(Y^\phi)' = c_1\Gamma_{\phi\phi\to YY}\frac{A^{\frac{1}{2}-3\omega_\phi}\Phi}{\mathbf{H}}\left(\frac{m_\phi^{\rm end}}{\langle E_Y\rangle^\phi}\right), \tag{12}$$

where

$$\mathbf{H} = \sqrt{\frac{\Phi}{A^{3\omega_\phi}} + \frac{R}{A} + \frac{Y^r\langle E_Y\rangle^r}{m_\phi^{\rm end}} + \frac{Y^\phi\langle E_Y\rangle^\phi}{m_\phi^{\rm end}}};$$
$$c_1 = \frac{\sqrt{3}M_p(1+\omega_\phi)}{(m_\phi^{\rm end})^2}. \tag{13}$$

A. Model of inflation

We will focus on a class of models called the α-attractor model [71,72], which unifies the large class of inflationary models parametrized by α and n. Here, we would like to mention that the canonical property of this class of models predicts inflationary observables (n_s, r) in favor of Planck observation [1,73]. The α-attractor E model has the defining inflaton potential,

$$V(\phi) = \Lambda^4\left[1 - e^{-\sqrt{\frac{2}{3\alpha}}\frac{\phi}{M_p}}\right]^{2n}, \tag{14}$$

where Λ is the mass scale that can be fixed by the CMB power spectrum, which is of the order of $\sim 8 \times 10^{15}$ GeV. Moreover, for $n = 1$, $\alpha = 1$, the α-attractor model turns out as the Higgs-Starobinsky model [74,75]. To this end, we would also like to point out that the recent Planck and BICEP/Keck combined result has put a constraint on the α to be $\sim(1\text{–}12)$ [76] within 1σ of the n_s value [77]. Throughout our study, we set $\alpha = 1$ and vary n. Importantly, we have checked that changing α within the aforementioned range does not significantly change our results. Let us first try to establish the relationship between the potential parameters with inflationary parameters. For the potential (14), the inflationary e-folding number N_k and tensor to scalar ratio r can be expressed as [78]

$$N_k = \frac{3\alpha}{4n}\left[e^{\sqrt{\frac{2}{3\alpha}}\frac{\phi_k}{M_p}} - e^{\sqrt{\frac{2}{3\alpha}}\frac{\phi_{\rm end}}{M_p}} - \sqrt{\frac{2}{3\alpha}}\frac{(\phi_k - \phi_{\rm end})}{M_p}\right],$$
$$r = \frac{64n^2}{3\alpha\left(e^{\sqrt{\frac{2}{3\alpha}}\frac{\phi_k}{M_p}} - 1\right)^2}. \quad (15)$$

Here, ϕ_k and $\phi_{\rm end}$ denote the values of the scalar field ϕ at the Hubble crossing of a particular mode k and the end of the inflation, respectively. From the condition of the end of the inflation $\epsilon_v(\phi_{\rm end}) = \frac{1}{2M_p^2}(V'(\phi_{\rm end})/V(\phi_{\rm end}))^2 = 1$, the value of the field and the potential at the end of the inflation are

$$\phi_{\rm end} = \sqrt{\frac{3\alpha}{2}}M_p \ln\left(\frac{2n}{\sqrt{3\alpha}} + 1\right), \quad V_{\rm end} = \Lambda^4\left(\frac{2n}{2n+\sqrt{3\alpha}}\right)^{2n}. \quad (16)$$

For a given canonical inflaton potential $V(\phi)$, the inflationary observables can be related to the slow-roll parameters and the Hubble parameter at the point when the mode with wave number k crosses the horizon,

$$n_s = 1 - 6\epsilon_v(\phi_k) + 2\eta_v(\phi_k), \qquad r = 16\epsilon_v(\phi_k),$$
$$H_k = \frac{\pi M_p\sqrt{rA_s}}{\sqrt{2}} \simeq \frac{V(\phi_k)}{3M_p^2}, \quad (17)$$

where the slow-roll parameters can be expressed as

$$\epsilon_v = \frac{M_p^2}{2}\left(\frac{V'(\phi)}{V(\phi)}\right)^2; \qquad |\eta_v| = M_p^2\frac{|V''(\phi)|}{V(\phi)}. \quad (18)$$

A_s is the amplitude of the inflaton fluctuation, which is measured from the CMB observation. The above Eq. (17) can be inverted to give the field value ϕ_k as

$$\phi_k = \sqrt{\frac{3\alpha}{2}}M_p \ln\left(1 + \frac{4n + \sqrt{16n^2 + 24\alpha n(1+n)(1-n_s)}}{3\alpha(1-n_s)}\right). \quad (19)$$

Plugging the above expression of ϕ_k into the H_k expression of (17), one can determine the mass scale Λ as

$$\Lambda = M_p\left(\frac{3\pi^2 rA_s}{2}\right) \times \left[\frac{2n(1+2n) + \sqrt{4n^2 + 6\alpha(1+n)(1-n_s)}}{4n(1+n)}\right]^{\frac{n}{2}}. \quad (20)$$

In order to solve the Boltzmann equations (12), one needs to replace the inflaton field variable in terms of its oscillation average, which can be further expressed in terms of the energy density of the inflaton. Such an average over oscillation period provides the following relation: $V(\phi(t)) = \rho_\phi(t)$ [79]. By using this, the effective mass m_ϕ of the inflaton can be expressed in terms of inflaton energy density during reheating as

$$m_\phi^2 = -\frac{4n\rho_\phi(\{1 - (\frac{\rho_\phi}{\Lambda^4})^{\frac{1}{2n}}\}^{-1} - 2n)}{3\alpha(\{1 - (\frac{\rho_\phi}{\Lambda^4})^{\frac{1}{2n}}\}^{-1} - 1)^2 M_p^2} \simeq 2n(2n-1)\lambda^{\frac{1}{n}}\rho_\phi^{\frac{n-1}{n}}, \quad (21)$$

under the assumption that the near the minima, the potential of the form of the α-attractor potential be $V(\phi) \simeq \lambda\phi^{2n}$. Where $\lambda = \Lambda^4(\sqrt{\frac{2}{3\alpha}}\frac{1}{M_p})^{2n}$. For $n = 1$ model, the inflaton mass turns out to be $m_\phi \simeq (2\Lambda^2)/(\sqrt{3\alpha}M_p)$. After identifying all of the required parameters during inflation, one can set initial conditions for subsequent reheating dynamics, which in turn provide important relationships among the reheating parameters, namely the reheating temperature $T_{\rm re}$ and e-folding number $N_{\rm re}$ in terms of (n_s, r). Therefore, we can establish the relations between the CMB anisotropy and reheating era via inflation.

B. Reheating parameters and observable constraints

In order to solve Boltzmann equations numerically, the initial conditions for the dimensionless comoving densities are set at the end of inflation,

$$\Phi(A=1) = \frac{3}{2}\frac{V_{\rm end}}{(m_\phi^{\rm end})^4},$$
$$R(A=1) = Y^r(A=1) = Y^\phi(A=1) = 0. \quad (22)$$

Combining Eqs. (16), (20), and (22), we can clearly see that the initial condition of the reheating dynamics strictly depends on the CMB parameters such as n_s, r, A_s, and the exponent of the potential n that, in turn, is related to the inflaton equation of state ω_ϕ following the relation $\omega_\phi = (n-1)/(n+1)$ [80] (for the potential of the form $\sim\phi^{2n}$). Throughout our analysis, we consider a fixed value of A_s, which is the central value of $A_s = 2.1 \times 10^9$ from Planck [81]. Furthermore, n_s and r can be related through Eq. (17). Therefore, reheating parameters such as the reheating temperature turns out to be a function of n_s, ω_ϕ, and the decay term Γ_ϕ. Once we solve the Boltzmann equations numerically during reheating, the reheating temperature can be identified at the point where the total interaction rate $\Gamma_T = \Gamma_\phi + \Gamma_{\phi\phi\to YY}$ satisfies the following condition:

$$H(A_{\rm re})^2 = \left(\frac{\dot{A}_{\rm re}}{A_{\rm re}}\right)^2 = \frac{\rho_\phi(\Gamma_\phi, A_{\rm re}, n_s) + \rho_r(\Gamma_\phi, A_{\rm re}, n_s) + \rho_Y(\Gamma_\phi, A_{\rm re}, n_s))}{3M_p^2} = \Gamma_T^2, \quad (23)$$

where $A_{\rm re} = a_{\rm re}/a_{\rm end}$ is the normalized scale factor at the end of reheating. To this end, let us point out that the above condition may not necessarily always be satisfied. For those situations, $\rho_\phi = \rho_R$, can be used. Such a situation may arise when the dilution of radiation due to expansion is faster than the production, which may happen for $\omega_\phi > 1/3$. We will discuss such scenarios in detail in our subsequent paper. Since the gravitational interaction rate is Planck suppressed [see, for instance, Eqs. (2)–(4)], at the point of reheating end, the gravitational production rate of the DM from inflaton is subdominant compared to the decay rate of the inflaton, $\Gamma_{\phi\phi\to YY}|_{A=A_{\rm re}} \ll \Gamma_\phi$. Therefore, we can safely approximate the total interaction rate at the end point of reheating as $\Gamma_T \simeq \Gamma_\phi$. This will be useful for our analytic computation of the reheating parameters. Furthermore, the reheating temperature can be expressed in terms of radiation temperature as

$$T_{\rm re} = T_{\rm rad}^{\rm end} = \left(\frac{30}{\pi^2 g_{\rm re}}\right)^{1/4} \rho_r(\Gamma_\phi, A_{\rm re}, n_s)^{1/4}. \quad (24)$$

We can also relate the reheating temperature to the present CMB temperature under the assumption that after reheating, entropy is preserved in the CMB and neutrino background today; that leads to the following constraint relation:

$$T_{\rm re} = \left(\frac{43}{11 g_{s,re}}\right)^{\frac{1}{3}} \left(\frac{a_0 T_0}{k}\right) H_k e^{-N_k} e^{-N_{\rm re}} = \mathcal{G} e^{-N_{\rm re}}, \quad (25)$$

$$\text{where } \mathcal{G} = \left(\frac{43}{11 g_{s,re}}\right)^{\frac{1}{3}} \left(\frac{a_0 T_0}{k}\right) H_k e^{-N_k}. \quad (26)$$

At the present CMB temperature, $T_0 = 2.725k$, the CMB pivot scale of Planck $k/a_0 = 0.05\ {\rm Mpc}^{-1}$, a_0 is the cosmological scale factor at present, and $g_{s,re}$ is the degrees of freedom associated with entropy at reheating. Utilizing Eqs. (23), (24), and (25), we can fix Γ_ϕ in terms of $T_{\rm re}$. Since $T_{\rm re}$ is a function of n_s, there must be a one-to-one correspondence between the parameters n_s, $T_{\rm re}$, and Γ_ϕ once we fixed ω_ϕ. Furthermore, cosmological observation on the DM abundance $\Omega_Y h^2$ provides a second constraint relation as [81,82]

$$\Omega_Y h^2 = m_Y \frac{(Y^r(A_F) + Y^\phi(A_F))}{R(A_F)} \frac{T_F A_F}{T_{\rm now} m_\phi^{\rm end}} \Omega_r h^2 = 0.12, \quad (27)$$

where the present day radiation abundance $\Omega_R h^2 = 4.3 \times 10^{-5}$ and T_F is the radiation temperature determined at a very late time A_F, when both comoving radiation and DM energy density became constant. Solving Boltzmann equations and utilizing the conditions mentioned in Eqs. (25) and (27), we can constrain the DM parameters $(\langle\sigma v\rangle, m_Y)$ in terms of $(T_{\rm re}, n_s)$. The DM particles produced from a radiation bath populated the early Universe with two possible mechanisms: 1) The produced DM particles reach thermal equilibrium, and as the temperature falls below the DM mass, the number density of DM freezes out. This mechanism is referred to as the freeze-out mechanism [83–90]. 2) The interaction of the DM particles with the radiation bath could be too weak to attain thermal equilibrium before it freezes out. This mechanism is referred to as the freeze-in [91] mechanism, and the produced DM particles are generally known as feebly interacting DM (FIMP) [17–26]. For gravitationally produced DM, the freeze-in mechanism will be effective, and DM produced from the radiation bath will have both possibilities of freeze-in and freeze-out production. However, we will consider the freeze-in mechanism for both the DM sector.

III. CONSTRAINING THE DARK SECTOR

As already emphasized in the beginning, the production of gravitational DM is an interesting, physically motivated scenario that needs detailed exploration. Following the references on gravitational DM [45–48,50], in this paper, we explore the observationally viable DM scenarios in terms of different inflationary models. Important reheating parameters, such as the equation of state ω_ϕ associated with the inflaton potential and reheating temperature $T_{\rm re}$, will play an important role in constraining the parameters such as the maximum possible mass of the DM. Moreover, since we consider the DM production from the radiation bath, we also place constraints on the average cross section times velocity $\langle\sigma v\rangle$. The dark sector may have different possibilities in terms of the nature of the DM and the number of components.

A. Single component DM

In our present framework, we have two different underlying production mechanisms. To understand the construction from each, one examines the evolution of different density components during reheating, as shown in Fig. 3. The production of DM components due to gravity mediation will naturally occur at the very beginning of the reheating phase when the inflation energy density is maximum, and this is depicted by the green curve. On the other hand, the DM production from the radiation bath will follow the evolution of radiation itself, which is depicted by a solid red curve. Therefore, maximum production will naturally occur near the end of reheating, as depicted by the solid black line. Finally, combining both the gravitational production and production from the radiation bath will contribute to the current DM abundance. An interesting aspect of such products of the same type of DM from two different mechanisms is that it will lead to a mixture of components with different velocity distribution, whose density perturbation may grow differently and provide distinct signatures in the small scale structure, which will be studied in our future publication.

Anyway, for the case of a purely gravity-mediated scenario, the mass of the DM is the only parameter. Therefore, in this scenario, reheating dynamics are controlled by two parameters (Γ_ϕ, m_Y) and two constraints relations Eqs. (25) and (27). Hence, the dynamics are determined completely by the inflation model under consideration instead of the nongravitational DM production scenario, which contains an annihilation cross section as an additional parameter. A large class of inflationary models such as α-attractor endows with a degenerate prediction of large scale observables, namely, scalar spectral index (n_s) and tensor to scalar ratio (r) but with distinguishing properties in terms of their effective inflaton equation of state ω_ϕ during reheating. Such degeneracy can be lifted during reheating, considering various other observables. For example, primordial gravitational waves encode distinct signatures depending on the reheating equation of state [92,93]. In our present analysis, also for a given equation of state ω_ϕ, solely gravitationally produced DM will assume a distinct value of its mass $m_Y^{\rm max}$ compatible with the DM abundance as can be seen in the Figs. 1 and 2, and the shaded yellow regions are the only allowed parameter plane that are either bounded by the value of $\omega_\phi \sim (0,1)$ or by the minimum $T_{\rm re}^{\rm min} \simeq 10^{-2}$ GeV set by the Big Bang nucleosynthesis (BBN) and maximum $T_{\rm re}^{\rm max} \simeq 10^{15}$ GeV set by the instantaneous reheating. Therefore, simple DM mass produced gravitationally during reheating can give valuable information about inflaton potential. An important point we should remember is that the condition $H = \Gamma_\phi$ leads to a unique reheating temperature $T_{\rm re}$ for a given n_s, and this is precisely the reason the present DM abundance is satisfied for a fixed DM mass. However, the suffix "max" in $m_Y^{\rm max}$ is due to the reason that this is the maximum possible DM mass in the ($\langle\sigma v\rangle$ Vs m_Y) plane that satisfies the abundance $\Omega_Y h^2 = 0.12$, when finite DM coupling with the radiation bath is included in the process; and it is in the limit $\langle\sigma v\rangle \to 0$, when $m_Y \to m_Y^{\rm max}$ as shown in Figs. 4 and 5. The generic expression of $m_Y^{\rm max}$ is derived as

$$m_Y^{\rm max} = \frac{\mathcal{G}\beta T_{\rm now}}{n_Y^{\rm re} A_{\rm re}^3}\left(\frac{\Omega_Y h^2}{\Omega_r h^2}\right)_{\rm now},$$
$$\text{where } A_{\rm re} = \left(\frac{12 M_p^2 H_{\rm end}^2 (1+\omega_\phi)^2}{\mathcal{G}^4 \beta (5-3\omega_\phi)^2}\right)^{\frac{-1}{(1-3\omega_\phi)}}. \quad (28)$$

The number density $n_Y^{\rm re}$ is calculated at the end of reheating with normalized scale factor $A_{\rm re}$ and associated expressions for each component are

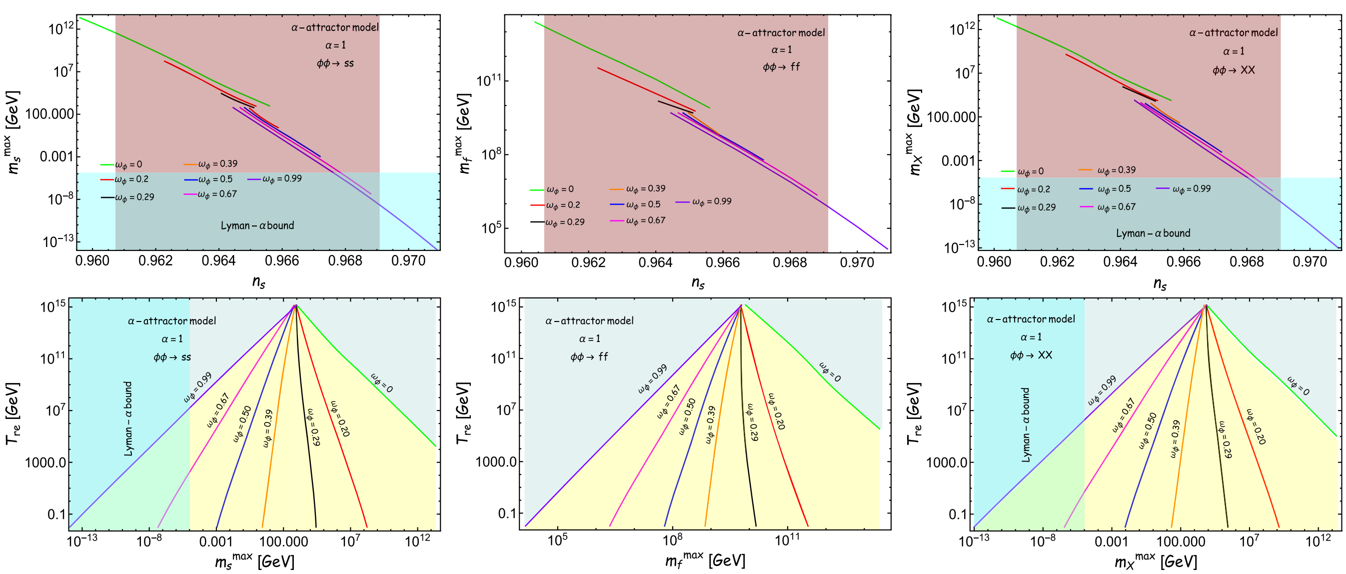

FIG. 1. Upper panel: The variation of the maximum allowed values of the DM mass $(m_Y^{\rm max})$ as a function of the scalar spectral index (n_s) corresponding to the fixed value of the DM abundance $\Omega_Y h^2 \simeq 0.12$ for the cases wherein $\omega_\phi = (0, 0.2, 0.29, 0.39, 0.5, 0.67, 0.99)$ (in green, red, black, orange, blue, magenta, and purple). We have considered the scenario where the α-attractor model describes the inflationary dynamics. We have indicated the 1-σ range of spectral index n_s (as the violet band) associated with the constraints from the Planck [1]. Further, the sky blue band corresponds to the DM masses lighter than 10 KeV, indicating the Lyman-α bound [67,94]. Lower panel: We have illustrated the variation of the reheating temperature as a function of the maximum allowed DM mass for seven different values of ω_ϕ covering the entire possible range of $\omega_\phi(0,1)$. Further, the yellow region shows the allowed parameters space, whereas the light green indicates the forbidden region.

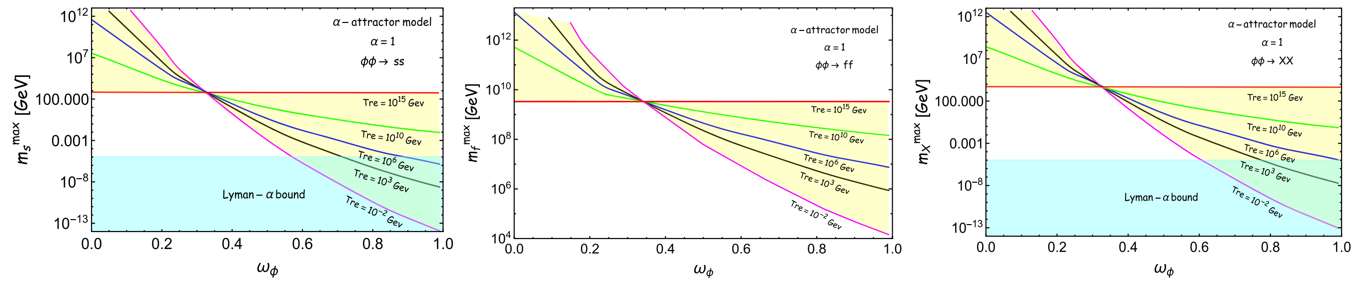

FIG. 2. The variation of the maximum allowed DM mass $m_Y^{\max}$ over a range of inflaton equation of state $\omega_\phi = (0, 1)$ for five different values of the reheating temperature $T_{\rm re} = (10^{-2}, 10^3, 10^6, 10^{10}, 10^{15})$ GeV (showed in magenta, black, blue, green, and red). The sky blue band indicates restriction from Lyman-α observations, and the yellow shaded region indicates the allowed parameters in $m_Y^{\max} - \omega_\phi$ plane.

$$
\begin{aligned}
n_X^{\rm re} &\approx \frac{3}{4096\pi}\frac{(1+\omega_\phi)}{(1+3\omega_\phi)}\left(\frac{H_{\rm end}}{A_{\rm re}}\right)^3,\\
n_s^{\rm re} &\approx \frac{3}{512\pi}\frac{(1+\omega_\phi)}{(1+3\omega_\phi)}\left(\frac{H_{\rm end}}{A_{\rm re}}\right)^3,\\
n_f^{\rm re} &\approx \frac{m_f^2 \lambda^{\frac{\omega_\phi-1}{\omega_\phi+1}}\nu(\omega_\phi)}{4096\pi(1+3\omega_\phi)(H_{\rm end}^2 M_p^2)^{\frac{2\omega_\phi}{1+\omega_\phi}}}\left(\frac{H_{\rm end}}{A_{\rm re}}\right)^3\\
&= \frac{3}{2048\pi}\frac{1+\omega_\phi}{1-\omega_\phi}\left(\frac{m_f}{m_\phi^{\rm end}}\right)^2\left(\frac{H_{\rm end}}{A_{\rm re}}\right)^3. \qquad (29)
\end{aligned}
$$

We should emphasize at this point that the above expression for the DM mass is sensitive to $(H_{\rm end}, \omega_\phi)$. Detailed derivation and the associated symbols of the above expressions are given in the Appendix A. Any value of the DM mass above $m_Y^{\max}$ is excluded because of overabundance. In Fig. 1, we have shown the allowed DM masses $m_Y^{\max}$ as a function of the spectral index and reheating temperature for different inflaton equations of state $\omega_\phi = (0, 0.2, 0.29, 0.39, 0.50, 0.67, 0.99)$ and assumed different single component DM species namely, scalar, fermion, and vector. Therefore, we cover the whole possible range of inflaton equation of states $\omega_\phi = (0, 1)$, and the allowed parameter space is shown by the shaded yellow region in the $(T_{\rm re} - m_Y^{\max})$ plane. It suggests that for the entire range of inflaton equations of state between (0, 1), the allowed mass of the scalar/vector DM must lie between $(1.2 \times 10^{-14}/9.6 \times 10^{-14}, 10^{13})$ GeV. And for the fermionic DM, the possible range turns out to be $(10^4, 10^{13})$ GeV. Here, one should notice the distinct mass range allowed for the DM for boson and fermion. Bosonic DM mass can be as low as in the eV range, which can be identified as an axionlike particle. It would be interesting to study in detail along this direction. Anyway, as has already been pointed out, there is a one to one correspondence between the DM mass and the reheating temperature; we provide possible constraints on the value of $(n_s, T_{\rm re}, m_Y^{\max})$ in terms of different inflaton equations of states in Table I. To determine the possible bound on the minimum value of the DM mass, we use the additional constraints arising from the Lyman-α forest dataset, which in turn imposes further restrictions on the inflationary and reheating parameters $(n_s, T_{\rm re})$. Additionally, in Fig. 2, we have shown the allowed DM mass as a function of the inflaton equation of state for different sets of reheating temperature. Interestingly, depending upon the inflaton equation of state, the allowed DM mass range changes and shrank to the same point corresponding to the maximum reheating temperature $T_{\rm re}^{\max} \sim 10^{15}$ GeV. This point also indicates the result for $\omega_\phi \to 1/3$ because for $\omega_\phi = 1/3$, reheating happens instantaneously with reheating

TABLE I. Different inflaton equation of state, associated bound on scalar spectral index (n_s), reheating temperature $T_{\rm re}$ (measured in units of GeV), and DM mass m_Y (measured in units of GeV), considering purely gravitational production of DM.

	$\omega_\phi = 0$			$\omega_\phi = 0.5$			$\omega_\phi = 0.99$		
Parameters	$\phi\phi \to SS$	$\phi\phi \to ff$	$\phi\phi \to XX$	$\phi\phi \to SS$	$\phi\phi \to ff$	$\phi\phi \to XX$	$\phi\phi \to SS$	$\phi\phi \to ff$	$\phi\phi \to XX$
$n_s^{\min}$	0.9596	0.9604	0.9601	0.9648	0.9648	0.9648	0.9645	0.9645	0.9645
$n_s^{\max}$	0.9656	0.9656	0.9656	0.9672	0.9672	0.9672	0.9676	0.9700	0.9680
$T_{\rm re}^{\min}$	1.8×10^4	3.5×10^5	1.1×10^5	10^{-2}	10^{-2}	10^{-2}	1.4×10^7	10^{-2}	1.5×10^6
$T_{\rm re}^{\max}$	10^{15}	10^{15}	10^{15}	10^{15}	10^{15}	10^{15}	10^{15}	10^{15}	10^{15}
$m_Y^{\max}$(min)	960	8.0×10^9	7.7×10^3	1.1×10^{-3}	6.1×10^7	9.0×10^{-3}	10^{-5}	1.4×10^4	10^{-5}
$m_Y^{\max}$(max)	$m_\phi^{\rm end}$	$m_\phi^{\rm end}$	$m_\phi^{\rm end}$	600	5.0×10^9	5.0×10^3	640	6.0×10^9	7.0×10^3

TABLE II. Different reheating temperatures, associated bound on inflaton equation state ω_ϕ, and DM mass m_Y (measured in units of GeV), considering only gravitationally produced DM.

	$T_{\rm re} = 10^{-2}$ GeV			$T_{\rm re} = 10^{3}$ GeV			$T_{\rm re} = 10^{10}$ GeV		
Parameters	$\phi\phi \to SS$	$\phi\phi \to ff$	$\phi\phi \to XX$	$\phi\phi \to SS$	$\phi\phi \to ff$	$\phi\phi \to XX$	$\phi\phi \to SS$	$\phi\phi \to ff$	$\phi\phi \to XX$
$\omega_\phi^{\rm min}$	0.11	0.15	0.13	0.05	0.09	0.07	0.0	0.0	0.0
$\omega_\phi^{\rm max}$	0.56	1.0	0.60	0.71	1.0	0.77	1.0	1.0	1.0
$m_Y^{\rm max}$ (min)	10^{-5}	1.4×10^4	10^{-5}	10^{-5}	8.7×10^5	10^{-5}	9.2×10^{-3}	1.4×10^8	7.0×10^{-2}
$m_Y^{\rm max}$ (max)	$m_\phi^{\rm end}$	$m_\phi^{\rm end}$	$m_\phi^{\rm end}$	$m_\phi^{\rm end}$	$m_\phi^{\rm end}$	$m_\phi^{\rm end}$	3.5×10^7	5.2×10^{11}	2.8×10^8

temperature $T_{\rm re} \sim 10^{15}$ GeV. The analytic expression of that specific mass [cf. Eqs. (28) and (29)] turned out to be dependent on the two factors, inflation energy scale $H_{\rm end}$ and inflaton equation of state ω_ϕ. Moreover, the possible bound on the inflaton equation of state and the mass of the DM for different sample values of reheating temperatures are shown in Table II.

When DM production from a radiation bath is included in the reheating process, Figs. 4 and 5 depict the region of the allowed cross section $\langle\sigma v\rangle$ in terms of n_s for two distinct values of the inflaton equations of state $\omega_\phi = (0, 0.5)$, respectively. It is clear from the figures that for finite cross sections with $m_Y < m_Y^{\rm max}$, the production from a radiation bath is always dominating compared to that of gravitational production. However, as one approach towards $m_Y^{\rm max}$,

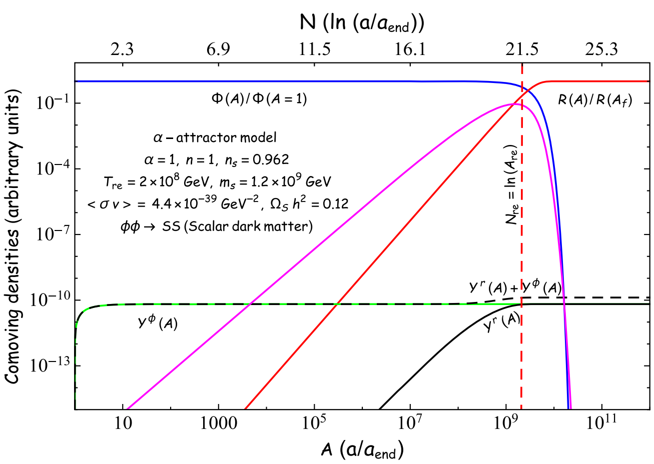

FIG. 3. We have plotted the evolution of the different energy components (inflaton, radiation) and the number density of DM as a function of the normalized scale factor (alternatively, the e-folding number is counting after the inflation) for the α-attractor model with $\alpha = 1$. The blue and red curve indicates the variation of the comoving densities of inflaton and radiation, respectively. Further, the black and green curve shows the evolution of the comoving number densities (Y^r, Y^ϕ) in arbitrary units produced from the radiation bath and the inflaton (mediated by gravity), accordingly. Moreover, the dotted black curve shows the evolution of the total comoving DM number density $(Y^r + Y^\phi)$, where we are taking into account both possibilities of the DM production.

gravity mediated DM production is increasingly dominated considering the fixed value of $\Omega_Y h^2 \simeq 0.12$. This fact entails the value of $\langle\sigma v\rangle$ approaching towards zero for not to overproduce the DM. Another important point is to note that for $m_Y > T_{\rm re}$, there always exists a maximum cross section for a given temperature once we fixed ω_ϕ. In the in-set of all the figures, we show how the cross section is approaching zero and gravitational DM contributes to the abundance. The last three plots of Figs. 4 and 5 also show the similar behavior in the $\langle\sigma v\rangle$ vs m_Y) plane near the maximum possible DM mass.

Due to the entropy conservation constraint, we generally observe that the reheating temperature is sensitive to the inflationary scalar spectral index n_s. The spectral index n_s is observationally bounded with a central value [1,77]. Because of this bounded region, one naturally obtains a limit on the reheating temperature. Furthermore, we get a different bound on this reheating temperature for different DM masses as all are intertwined through the reheating dynamics and inflationary dynamics. For example, from Fig. 4, for $\omega_\phi = 0$ $(\omega_\phi < \omega_r)$, the upper bound on the reheating temperature turns out as $T_{\rm re}^{\rm max} \simeq (4.9 \times 10^{11}, 4.0 \times 10^{12})$ GeV for scalar and vector DM, respectively, with $m_{s/X} = 10^6$ GeV, and $T_{\rm re}^{\rm max} \simeq 1.4 \times 10^{13}$ GeV for fermionic DM with $m_f = 5 \times 10^{10}$ GeV. However, for $\omega_\phi = 0.5 > 1/3$, one obtains $T_{\rm re}^{\rm min} \simeq (1.6 \times 10^7, 2.8 \times 10^4)$ GeV for scalar and vector DM with $m_{s/X} = 1$ GeV and $T_{\rm re}^{\rm min} \simeq 3 \times 10^6$ GeV for fermionic DM with $m_f = 5 \times 10^8$ GeV. In addition to that, the lower limit on the scalar spectral index is set by the BBN temperature for those models where $\omega_\phi < 1/3$ and instantaneous reheating for $\omega_\phi > 1/3$. In the allowed range of n_s, the cross section can not be arbitrarily large due to unitarity limit on the cross section $\langle\sigma v\rangle_{\rm max} = 8\pi/m_Y^2$. This will further constraint n_s and $T_{\rm re}$. For the $n = 1$ model, the lower limit on the scalar spectral index is modified due to the perturbative unitarity limit on the cross section. Moreover, the modification on the lower limit of n_s changes the minimum allowed value of the reheating temperature, such as for $\omega_\phi = 0$, $T_{\rm re}^{\rm min} \simeq (180, 6.4 \times 10^6)$ GeV for scalar/vector $(m_{s/X} = 10^6$ GeV) and fermionic DM $(m_f = 5 \times 10^{10})$, respectively.

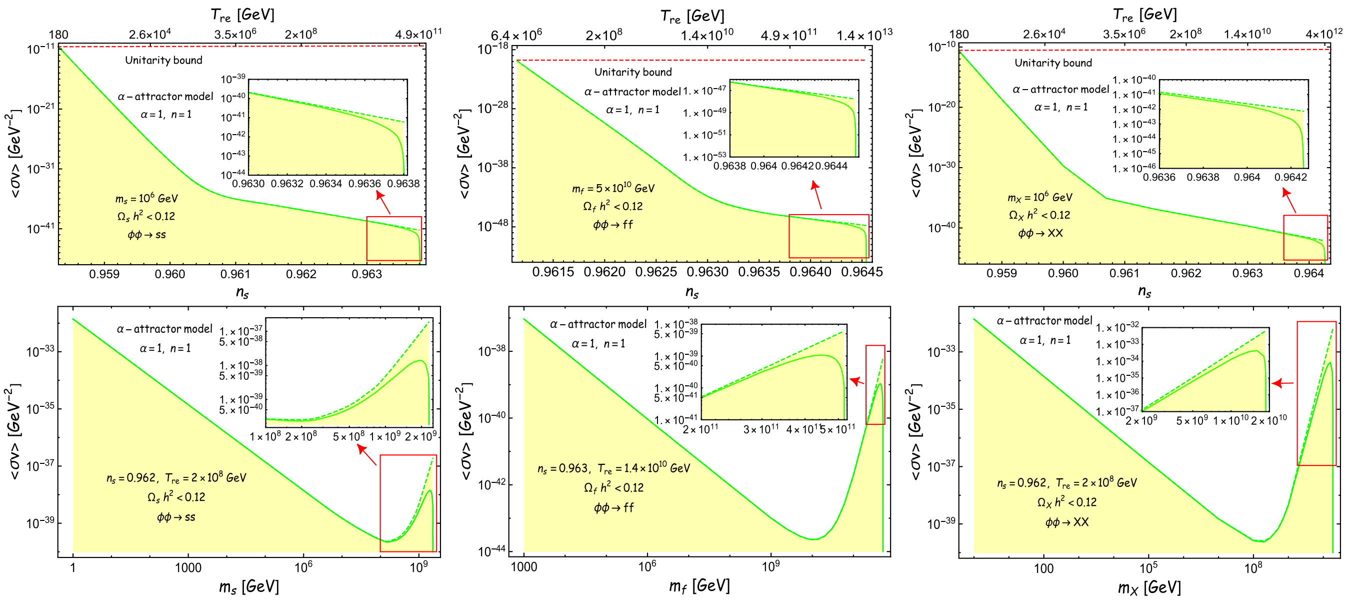

FIG. 4. Upper panel: $\langle\sigma v\rangle$ vs n_s plotted for three different gravitationally produced DM scenarios: $\phi\phi \to SS$ (scalar DM), $\phi\phi \to ff$ (fermionic DM), and $\phi\phi \to XX$ (vector DM) considering the α-attractor model with $\alpha = 1$, $n = 1$ (Higgs-Starobinsky model). The yellow shaded region corresponds to the DM abundance $\Omega_Y h^2 \leq 0.12$. The dashed green line implied the results when we took into account one possibility: DM production from a radiation bath with cross section $\langle\sigma v\rangle$, and the solid green line corresponds to both possibilities—DM can be produced from the scattering of inflatons gravitationally and from the radiation bath. The lower limit on the spectral index is given by the perturbative unitarity limit of the cross section $\langle\sigma v\rangle_{\rm max} = \frac{8\pi}{m_Y^2}$ (shown by the red dashed line), whereas the upper limit is associated with that particular value of the spectral index or reheating temperature when only gravitational production of the DM is sufficient to produce the correct relic of the DM. So any value of n_s above this is excluded because this leads to an overabundance. Lower panel: Variation of $\langle\sigma v\rangle$ as a function of DM mass m_Y. The upper limit on DM mass is associated with that particular value of the DM mass $m_Y^{\rm max}$ when only the gravitational production of the DM is sufficient to produce the correct relic.

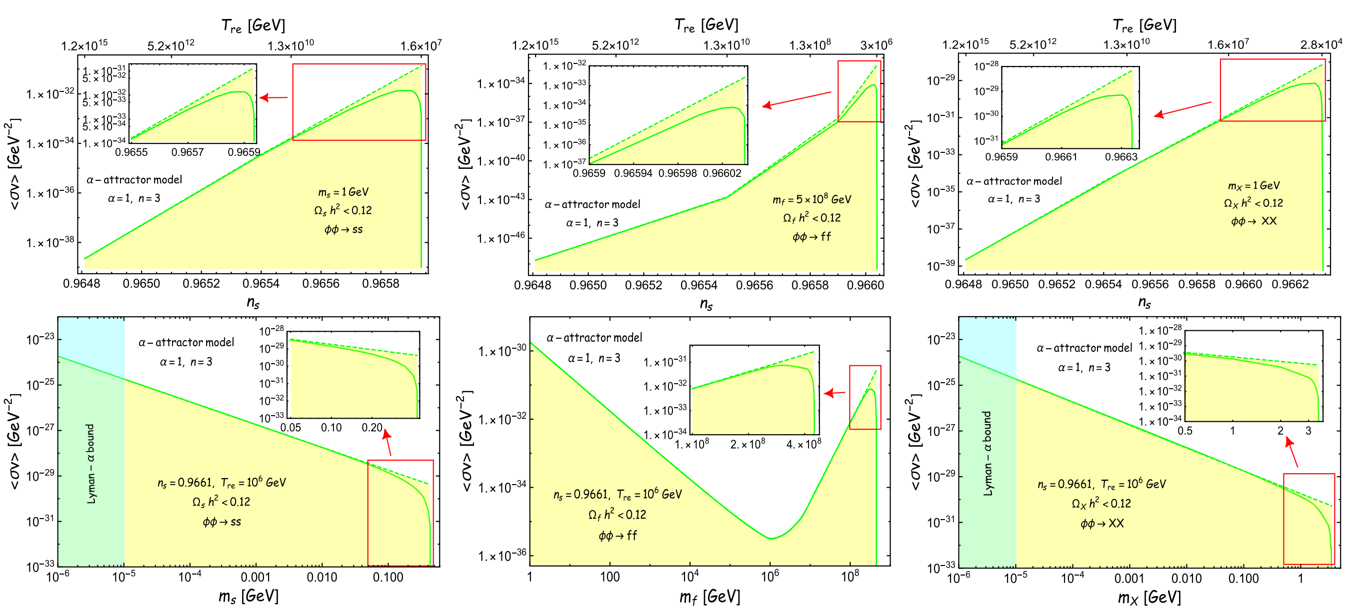

FIG. 5. Upper panel: $\langle\sigma v\rangle$ vs n_s, the description of this figure is the same as previous Fig. 4; the main difference is that here we have plotted for α-attractor model with $\alpha = 1$ and $n = 3$. In addition to that, the lower limit on the spectral index corresponds to instantaneous reheating ($N_{\rm re} \to 0$). Lower panel: $\langle\sigma v\rangle$ vs m_Y, the description of this figure is the same as previous Fig. 4. The sky blue band indicates restriction from Lyman-α observations.

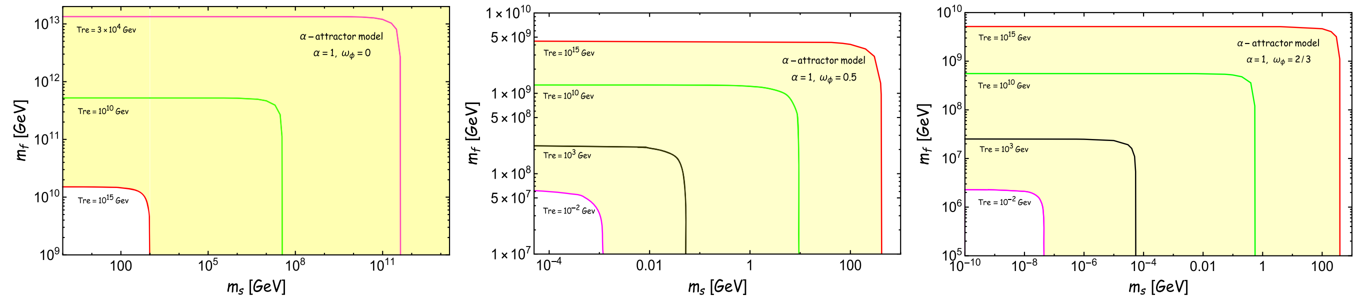

FIG. 6. *Two-component DM scenario*: m_f vs m_s were plotted for three different values of inflaton equations of state $\omega_\phi = (0, 0.5, 2/3)$ considering different reheating temperatures (shown by different colored lines). Those lines corresponds to the fixed value of the present DM abundance $\Omega_{X(s+f)}h^2 \simeq 0.12$. For all the cases, we consider purely gravitationally produced DM. The DM sector consists of two sectors, one for scalar and another one for fermionic DM. Here, the α-attractor model with $\alpha = 1$ describes the inflationary dynamics, and the yellow shaded region shows the allowed DM masses.

IV. TWO-COMPONENT DM

For the sake of completeness, in this section, we will briefly discuss the two-component DM scenario and the constraints on the parameter space. We explore possible allowed mass ranges when it is produced gravitationally. Since the behavior of scalar and vector DM is qualitatively the same, we assume the present-day abundance of total DM is composed of scalar and fermionic type particles. The dynamical equation will be the same as previously discussed in Eqs. (5)–(8), with no production from the radiation bath. From Fig. 6, it is clear that not all the range of the mass is allowed, and as expected, it is explicitly dependent upon the reheating equation of state or rather types of the inflaton potential near its minimum. For each plot, the yellow shaded region is the allowed parameter space if we include all possibilities of reheating temperature. The region is either bounded by the maximum reheating temperature $\sim 10^{15}$ GeV, and the BBN bound 10^{-2} GeV, or by $m_Y^{\rm max}$ discussed in the previous section.

An interesting observation of this analysis is that there exists a one-to-one correspondence between scalar and fermionic DM masses. For a fixed combination of $(T_{\rm re}, \omega_\phi)$, we can uniquely determine the mass of one component once another component is fixed. The maximum allowed mass for any one component is associated with the single component DM scenario, which we already discussed earlier. However, the minimum value of the mass approaches zero as the system starts dominating by only one component, either scalar or fermionic DM.

V. COMPARISON ON GRAVITATIONAL DM PRODUCTION FROM INFLATON AND RADIATION BATH

In our discussions so far, we considered gravitational DM production purely from the inflaton annihilation. However, in principle, gravitational production from the radiation bath will contribute, which we mentioned before, to be subleading compared to the production from inflaton. This section will show through an explicit calculation that this is indeed the case. For the case of s-channel gravitational DM production from inflaton we have production rates in Eqs. (2)–(4). The production of gravitational DM from the radiation bath during reheating has already been studied [26,54–56], and the interaction rate per unit physical volume is expressed as

$$R(T) = \gamma \frac{T^8}{M_p^4}, \tag{30}$$

where $\gamma = 1.9 \times 10^{-4}$ for scalar DM, $\gamma = 1.1 \times 10^{-3}$ for fermionic DM, or $\gamma = 2.3 \times 10^{-3}$ for vector DM. In addition to usual inflaton and the DM component from inflation, we have modified radiation dynamics and an additional DM production channel from radiation bath as follows:

$$\dot{\rho}_r + 4H\rho_r - \Gamma_\phi \rho_\phi (1 + \omega_\phi) + R(T)\langle E_Y \rangle^r = 0, \tag{31}$$

$$\dot{n}_{Y(R)} + 3H n_{Y(R)} - R(T) = 0, \tag{32}$$

where $n_{Y(R)}$ is the DM number density produced from the radiation bath due to gravitational interaction.

Now let us compare the results for DM production from a radiation bath mediated by gravity with the production from inflaton. The associated expressions for comoving DM number density in terms of reheating temperature calculated at the end of reheating for different types of DM, produced from either inflaton or radiation bath are (see Appendixes A and C)

$$\begin{aligned} n_s^{\rm re} A_{\rm re}^3 &\approx 8 n_X^{\rm re} A_{\rm re}^3 \approx \frac{3}{512\pi} \frac{(1+\omega_\phi)}{(1+3\omega_\phi)} \frac{\beta^2 T_{\rm re}^8 e^{6N_{\rm re}(1+\omega_\phi)}}{9 M_p^4 H_{\rm end}}, \\ n_f^{\rm re} A_{\rm re}^3 &\approx \frac{3}{2048\pi} \frac{1+\omega_\phi}{1-\omega_\phi} \left(\frac{m_f}{m_\phi^{\rm end}}\right)^2 \frac{\beta^2 T_{\rm re}^8 e^{6N_{\rm re}(1+\omega_\phi)}}{9 M_p^4 H_{\rm end}}, \\ n_{Y(R)}^{\rm re} A_{\rm re}^3 &\approx \frac{2\gamma}{3(1-\omega_\phi)} \frac{e^{\frac{3}{2}N_{\rm re}(3+\omega_\phi)} T_{\rm re}^8}{M_p^4 H_{\rm end}}. \end{aligned} \tag{33}$$

To derive the above equation, we use the following approximate relation: $H_{\rm re}^2 = \rho_R^{\rm re}/3M_p^2 = \beta T_{\rm re}^8/(3M_p^2) = H_{\rm end}^2 A_{\rm re}^{-3(1+\omega_\phi)}$, which indicates that at the end of reheating the Universe is dominated by radiation. The DM production from a radiation bath is maximum when the radiation temperature is maximum, which is approximately equivalent to taking $N_{\rm re} = 0$. Therefore, it would be sufficient to compare the above comoving densities for a different production channel at the point of instantaneous reheating,

$$n_R^s = \frac{n_s^{\rm re} A_{\rm re}^3}{n_{Y(R)}^{\rm re} A_{\rm re}^3} = \left(\frac{3}{512\pi}\frac{(1+\omega_\phi)}{(1+3\omega_\phi)}\frac{\beta^2}{9}\right) \times \left(\frac{3(1-\omega_\phi)}{2\gamma}\right) \tag{34}$$

$$n_R^f = \frac{n_f^{\rm re} A_{\rm re}^3}{n_{Y(R)}^{\rm re} A_{\rm re}^3} = \left(\frac{3}{2048\pi}\frac{(1+\omega_\phi)}{(1-\omega_\phi)}\frac{\beta^2}{9}\left(\frac{m_f}{m_\phi^{\rm end}}\right)^2\right) \times \left(\frac{3(1-\omega_\phi)}{2\gamma}\right). \tag{35}$$

From the above two equations, it can be checked that for any ω_ϕ, $n_R^s \gg 1$ [cf. Eq. (33)]. Hence, comoving DM number density for scalar/vector produced from inflaton always dominates over the production from the radiation bath. However, a fermionic DM dominating production channel is crucially dependent on $(m_f/m_\phi^{\rm end})$. For example, if the reheating is instantaneous and the value of the fermionic DM mass produced from inflaton assumes $m_f \simeq 10^{-3} m_\phi^{\rm end}$, then $n_R^f \ll 1$, which makes $n_f^{\rm re}$ subdominant compared to $n_{Y(R)}^{\rm re}$. If we convert this into reheating temperatures, it can be easily shown that above $T_{\rm re} \gtrapprox 10^{13}$ GeV, the production of fermionic DM from radiation bath will always dominate over the production from inflaton field, and it is less sensitive to the inflaton equation of state (see Fig. 7). In Fig. 7, solid lines correspond to gravitational DM production from inflaton scattering, and dotted lines correspond to DM production from both inflaton as well as a radiation bath. The light red shaded region within $10^{15} \gtrsim T_{\rm re} \gtrsim 10^{13}$ GeV clearly shows that the production from the inflaton field is subleading compared to that from the radiation bath. Depending upon the reheating equation of state, the mass range of the fermionic dark matter is observed to be slightly different.

So far, we have discussed DM production and its intimate connection with the inflationary and reheating phase. However, DM abundance does not contain much information about the nature of DM and its underlying production mechanism. In the subsequent discussions, we will focus more on the microscopic properties of DM, such as its phase-space distribution, free streaming lengths, etc. These properties play a significant role in the subsequent cosmological evolution of DM perturbation, which is deeply connected with the large-scale structure formation.

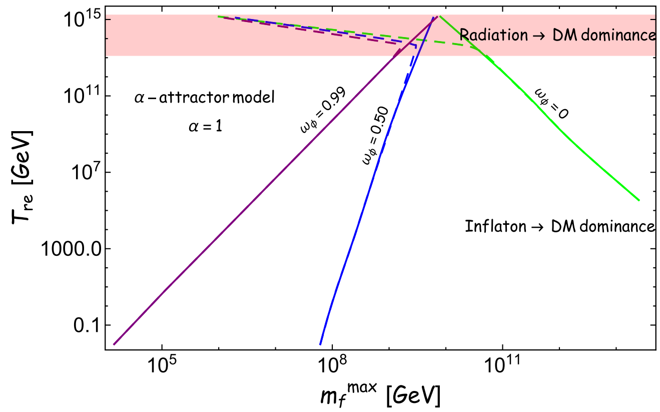

FIG. 7. Variation of reheating temperature as a function of DM mass for two different gravitationally produced DM scenarios: (1) DM generated only from inflaton scattering (shown in solid line) (2) We took the contribution from inflaton as well as SM scattering (shown in dashed line). These results are for fermionic DM with three different inflaton equations of state $\omega_\phi = (0, 0.5, 0.99)$. Furthermore, the light red band indicates the dominating contribution in the DM relic from the thermal bath over inflaton scattering.

VI. PHASE SPACE DISTRIBUTION OF GRAVITATIONALLY PRODUCED DM

In this section, we study the evolution of phase space distribution of DM, which will be observed to encode not only the underlying production mechanism but also the very nature of the DM itself. The DM production is purely gravitational and produced from inflaton through the process $\phi\phi \to SS/XX/ff$ for scalar (S), vector (X), and fermion (f), mediated by gravity. Gravitational production from a radiation bath will not be considered unless otherwise stated. The phase-space distribution (f_Y) of DM is evolved by the Boltzmann transport equation as

$$\frac{\partial f_Y}{\partial t} - H|\mathbf{p}_Y|\frac{\partial f_Y}{\partial |\mathbf{p}_Y|} = c[f_Y(|\mathbf{p}_Y|, t)], \tag{36}$$

where $c[f_Y(|\mathbf{p}|, t)]$ symbolizes the collision term, determined through an inflaton-DM interaction. Let us first calculate the collision term for this process. To calculate collision term, one of the important quantities is the phase space distribution of inflaton. The inflaton field is homogeneous in nature, and the phase space distribution of the inflaton field can be effectively written as $f_\phi(k, t) = (2\pi)^3 n_\phi(t)\delta^{(3)}(\mathbf{k})$, where, n_ϕ is the number density of the zero momentum inflaton particles. The required collision term for the transport equation is given by

$$\begin{aligned} c[f_Y(|\mathbf{p}_Y|,t)] &= \frac{1}{2p_{Y_0}}\int \frac{d^3\mathbf{k}}{(2\pi)^3 2k_0}\frac{d^3\mathbf{k}'}{(2\pi)^3 2k'_0}\frac{g_{Y'}d^3\mathbf{p}_{Y'}}{(2\pi)^3 2p_{Y'_0}}(2\pi)^4\delta^{(4)}(k+k'-p_Y-p_{Y'}) \\ |\mathcal{M}|^2_{\phi\phi\to YY'}f_\phi(k)f_\phi(k')[1\pm f_Y(p_Y)\pm f_{Y'}(p_{Y'})] &= \frac{\pi n_\phi(t)^2}{p_{Y_0}}\int \frac{1}{4m_\phi^2}\frac{g_{Y'}d^3\mathbf{p}_{Y'}}{2p_{Y'_0}}\delta(2m_\phi - p_{Y_0}-p_{Y'_0})\delta^{(3)}(\mathbf{p}_{Y'}+\mathbf{p}_Y) \\ |\mathcal{M}|^2_{\phi\phi\to YY'}[1\pm f_Y(p_Y)\pm f_{Y'}(p_{Y'})] &= \frac{\pi n_\phi(t)^2}{8g_Y p_{Y_0}p_{Y'_0}}\frac{g_Y g_{Y'}|\mathcal{M}|^2_{\phi\phi\to YY'}}{m_\phi^2}\delta(2m_\phi - p_{Y_0}-p_{Y'_0})[1\pm f_Y(p_Y)\pm f_{Y'}(p_{Y'})], \end{aligned} \tag{37}$$

where $(+)$ and $(-)$ sign, in the third bracket, are for bosonic and fermionic DM, respectively. g_y, $g_{Y'}$ represents the number of internal degrees of freedom for Y and Y'. Moreover, in the absence of Bose condensation or fermionic degeneracy, one may approximate the blocking and stimulated emission factor as $[1\pm f_Y(p_Y)\pm f_{Y'}(p_{Y'})]\simeq 1$. Furthermore, the corresponding gravitational DM production rate for the process $\phi\phi\to YY$ can be related with spin-averaged squared amplitude $|\mathcal{M}|^2_{\phi\phi\to YY}\to|\overline{M}|^2_{\phi\phi\to YY} = \sum_{\text{avg over initial pol}}\sum_{\text{sum over final pol}}\mathcal{M}|^2_{\phi\phi\to YY}$ [sum over the polarizations (spins) of the final particles and average over the polarizations (spins) of the initial ones] as

$$\Gamma_{\phi\phi\to YY} = n_\phi\frac{g_Y^2|\mathcal{M}|^2_{\phi\phi\to YY}}{32\pi m_\phi^2}\sqrt{1-\frac{m_Y^2}{m_\phi^2}}\simeq n_\phi\frac{g_Y^2|\mathcal{M}|^2_{\phi\phi\to YY}}{32\pi m_\phi^2}, \tag{38}$$

where we use the approximation $m_Y < m_\phi$. Therefore, combining Eqs. (37) and (38) and acknowledging the approximations mentioned above, the collision term takes the form,

$$\begin{aligned} c[f_Y(p_Y,t)] &\simeq \frac{2\pi^2 n_\phi(t)}{g_Y p_{Y_0}^2}\Gamma_{\phi\phi\to YY}\delta(m_\phi - p_{Y_0}) \\ &= \frac{2\pi^2 n_\phi(t)}{g_Y p_{Y_0}^3 H}\Gamma_{\phi\phi\to YY}\delta(t-t'), \end{aligned} \tag{39}$$

where t' is the cosmic time when p_Y is equal to the inflaton mass which satisfies the relation $p_Y a(t) = a(t')m_\phi$. The energy associated with each DM particle is $p_{Y_0} = m_\phi$. Upon substituting the above collision term into the transport equation (36), one obtains the DM phase space distribution as

$$f_Y(p_Y,t) = \frac{2\pi^2 n_\phi(t')}{g_Y m_\phi^3 H(t')}\Gamma_{\phi\phi\to YY}(t')\theta(t-t'). \tag{40}$$

Inflaton energy density during reheating can be evaluated by integrating Eq. (5), which leads to

$$\rho_\phi(t') = \rho_\phi^{\text{end}}A(t')^{-3(1+\omega_\phi)}e^{-\Gamma_\phi(t'-t_{\text{end}})}. \tag{41}$$

Here, we ignore the effect of DM production on the inflaton energy density as it is negligible compared to the production of radiation. The subscript "end" indicates the end of the inflation. We can write the above equation (41) for the inflaton energy density in terms of the inflaton energy density at the end of the reheating (ρ_ϕ^{re}) as

$$\rho_\phi(t') = \rho_\phi^{\text{re}}\left(\frac{A(t')}{A_{\text{re}}}\right)^{-3(1+\omega_\phi)}e^{-\Gamma_\phi(t'-t_{\text{re}})}. \tag{42}$$

As most of the region during reheating is dominated by the inflaton equation of state (EoS), we can approximate the scale factor as $a\propto t^{2/3(1+\omega_\phi)}$ and $t' = t_{\text{re}}(\frac{A(t')}{A_{\text{re}}})^{3(1+\omega_\phi)/2}$. Further, at the end of the reheating, when $t_{\text{re}} = \Gamma_\phi^{-1}$, the Hubble parameter $H_{\text{re}}\simeq\Gamma_\phi$ and the inflaton energy density approximately equals to the radiation energy density $\rho_\phi\simeq\rho_r = \frac{\pi^2}{30}g_{\text{re}}T_{\text{re}}^4$. Under these approximations, $\rho_\phi(t')$ assumes following form:

$$\rho_\phi(t') = \frac{\pi^2}{30}g_{\text{re}}T_{\text{re}}^4\left(\frac{A(t')}{A_{\text{re}}}\right)^{-3(1+\omega_\phi)}e^{1-(\frac{A(t')}{A_{\text{re}}})^{3(1+\omega_\phi)/2}}. \tag{43}$$

In the same way, Hubble parameter during reheating phase turns out as

$$H(t')\simeq H_{\text{re}}\left(\frac{A(t')}{A_{\text{re}}}\right)^{-\frac{3}{2}(1+\omega_\phi)}\simeq\Gamma_\phi\left(\frac{A(t')}{A_{\text{re}}}\right)^{-\frac{3}{2}(1+\omega_\phi)}. \tag{44}$$

Substituting Eqs. (43) and (44) into the phase-space distribution equation (40), one obtains the following form of the DM phase space distribution during reheating phase as

$$\begin{aligned} f_Y(p_Y,t) = {}& \frac{\pi^4 g_{\text{re}}}{15 g_Y\Gamma_\phi}\left(\frac{T_{\text{re}}}{m_\phi^{\text{end}}}\right)^4\left(\frac{m_\phi^{\text{end}}}{m_\phi(t')}\right)^4\left(\frac{A(t')}{A_{\text{re}}}\right)^{-\frac{3}{2}(1+\omega_\phi)} \\ & \times e^{1-(\frac{A(t')}{A_{\text{re}}})^{\frac{3}{2}(1+\omega_\phi)}}\Gamma_{\phi\phi\to YY}(t')\theta(t-t'). \end{aligned} \tag{45}$$

Instead of symbolizing the inflaton's mass by m_ϕ, we use $m_\phi(t)$ as the effective mass of the inflaton being a function

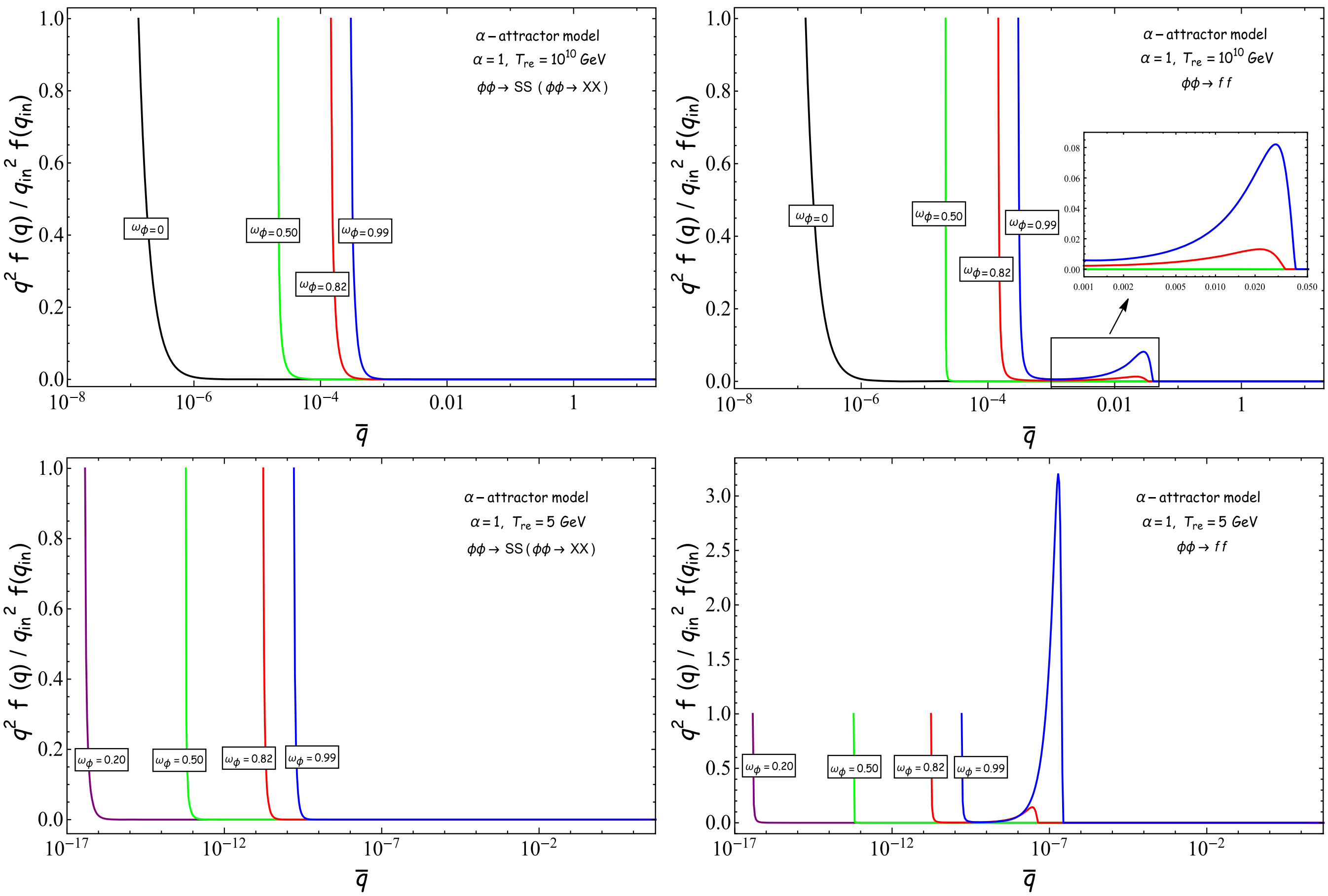

FIG. 8. The rescaled momentum distribution function of DM as a function of q, defined in Eq. (47), indicates rescaled comoving momentum for time-independent inflaton mass $[V(\phi) \sim \phi^2]$ with a few different inflaton equations of state $\omega_\phi = (0, 0.2, 0.5, 0.82, 0.99)$ (shown in different color) with two specific values of the reheating temperature $T_{\rm re} = (10^{10}, 5)$ GeV. On the left, we have plotted results for gravitationally produced scalar ($\phi\phi \to SS$) or vector DM ($\phi\phi \to XX$) and on the right for gravitationally produced fermionic DM ($\phi\phi \to ff$).

of time, and its evolution is followed by Eq. (21). To get a better approximation for the momentum distribution function $f_Y(p_Y, t)$, we have to calculate Eq. (40) by solving the sets of Boltzmann equations (5)–(8) numerically. The numerical solution of the rescaled momentum distribution function $f(q)$ is shown in Fig. 8; the form of $f(q)$ is defined in the following manner:

$$f_Y(p_Y, t) d^3 p = \frac{\pi^4 g_{\rm re}}{15 g_Y} \left(\frac{T_{\rm re}}{m_\phi^{\rm end}}\right)^4 \left(\frac{T_*}{a}\right)^3 f(q) d^3 q, \tag{46}$$

where q is the rescaled comoving momentum of the DM, which is defined as

$$q = \frac{pa(t)}{T_*} = \frac{A(t')}{A_{\rm re}} \frac{m_\phi(t')}{m_\phi(t_{\rm re})} = \bar{q} \frac{m_\phi(t')}{m_\phi(t_{\rm re})}. \tag{47}$$

Here, T_* is the time-independent quantity, defined as $T_* = m_\phi(t_{\rm re}) a_{\rm re}$. As can be observed from the Fig. 8, the phase space distribution function of DM naturally contains peaks at the initial time of reheating when most of the DM particles are produced gravitationally via scattering of inflatons, and the momentum of those produced particles should be around the mass of the inflaton. The characteristics of the peak and location will certainly be dependent on the background dynamics determined by the inflaton equation of state ω_ϕ and reheating temperature $T_{\rm re}$ as one can imagine that this characteristic peak will naturally be imprinted on the subsequent evolution of DM structures. In addition, the free streaming properties of DM will help understand the formation of the DM structure, and we will discuss this in detail in the following section. Furthermore, it can be observed that there exists a secondary peak in the fermionic distribution function at an even higher momentum, which arises due to nontrivial mass dependence in the fermionic annihilation rate $\Gamma_{\phi\phi\to ff} \propto \rho_\phi / m_\phi$ and consequently, the phase space distribution $q^2 f_f(q,t) \propto (a^2 \rho_\phi^2)/(m_\phi^3 H) \propto a^{\frac{1}{2}(5-9\omega_\phi)}$, as opposed to the bosonic phase-space distribution function $q^2 f_s(q,t) \propto (a^2\rho_\phi^2)/(m_\phi H) \propto a^{-\frac{1}{2}(5+3\omega_\phi)}$. Therefore, in the case of fermionic

DM, for $\omega_\phi > 5/9$, the phase space distribution function increases till the point when inflaton mass is equal to the mass of the DM ($m_Y = m_\phi$), and after that point, the distribution function approaches zero as the DM production is kinematically forbidden ($\Gamma_{\phi\phi\to YY} \to 0$) in the region where $m_\phi < m_Y$. The important point is to note that the peak value associated with the secondary peak increases as we $T_{\rm re}$ decreases, which increases the time elapsed to reach the point $m_\phi = m_Y$. However, for bosonic DM, such a secondary peak does not arise as $q^2 f_s(q,t)$ drops with a scale factor during reheating for a viable range of ω_ϕ, $0 \le \omega_\phi \le 1$. It would be interesting to look into this secondary peak and its physical significance in detail.

VII. MOMENTUM, FREE STREAMING LENGTH, AND CONSTRAINTS

We have already observed that the DM phase-space distribution peak occurs near the beginning of reheating, where the gravitational production of DM from inflaton is maximum. The momentum around that peak will also be maximum, which is $\sim m_\phi^{\rm end}$, which naturally depends on the inflaton equation of state. The obvious physical effect of this large initial momentum of the DM would be on their free streaming properties, which will have a significant impact on the perturbation evolution at a small scale. Large initial momentum will naturally suppress the structure formation at small scales. In this section, we will study this in detail and evaluate the possible constraints on the present DM velocity from the well-known Lyman-α bound on the DM mass for warm dark matter (WDM) [60–66]. If DM has no interaction with itself or with the SM particles, the momentum of the DM particles is redshifted by the expansion of the Universe. Therefore, we can relate the present momentum of the DM with the mean initial momentum at the time of its production as, $p_{\rm now} = (a_{\rm in}/a_{\rm now})p_{\rm in}$. For example, if the DM particles produced from the thermal bath, the mean initial momentum would assume $p_{\rm in} \sim 3T_{\rm re}$ at a scale factor $a_{\rm in} = a_{\rm re}$, and assuming the entropy being conserved between the end of reheating to today, the momentum at present would be calculated as

$$p_{\rm now} = \left(\frac{387}{11 g_{s,re}}\right)^{1/3} T_0, \tag{48}$$

where the present CMB temperature $T_0 = 2.725k = 2.3 \times 10^{-13}$ GeV and the $g_{s,re}$ is the effective number of degrees of freedom for entropy at reheating temperature. Now, by using the various experimental constraints on the WDM, such as the MCMC analysis of the XQ-100 and HIRES/MIKE Lyman-α forest datasets constraints, the mass of the WDM particle $m_{\rm wdm} > 5.3$ keV at 2σ range [64]. In Refs. [60,95], using the same Lyman-α forest dataset, the authors obtained the bound on $m_{\rm wdm} > 3.3$ keV using HIRES/MIKE and > 3.95 keV using SDSSIII/BOSS. Considering the overall conservative estimate of $m_{\rm wdm} > 3.9$ keV and $g_{s,re} \sim 100$, using Eq. (48), one gets the lower bound on the present DM velocity $v_{\rm dm} < 4.1 \times 10^{-8}$. Now using the above bounds on the WDM mass, we will first estimate the DM velocity for different production scenarios described so far.

Production from inflaton: For the gravitational DM produced from the inflaton, the initial momentum at production can be approximately taken to be $p_{\rm in} \sim m_\phi$, and the radiation temperature correspond to the scale factor $a = a_{\rm in}$ can be taken as the maximum radiation temperature $T_{\rm rad}^{\rm max}$. The radiation energy density will evolve as $\rho_r \propto T_{\rm rad}^4 \propto a^{-\frac{3(1+\omega_\phi)}{2}}$ [96]. Accumulating all the above expressions, one can find the present value of the DM momentum as

$$\begin{aligned} p_{\rm now} &= \frac{a_{\rm in}}{a_{\rm re}}\frac{a_{\rm re}}{a_{\rm now}} m_\phi \\ &= \left(\frac{43}{11 g_s(T_{\rm re})}\right)^{1/3} \frac{T_{\rm now}}{T_{\rm re}} \left(\frac{T_{\rm re}}{T_{\rm rad}^{\rm max}}\right)^{\frac{8}{3(1+\omega_\phi)}} m_\phi. \end{aligned} \tag{49}$$

Moreover, in the perturbative reheating scenario, the approximated analytical expression of the maximum radiation temperature $T_{\rm rad}^{\rm max}$ can be written as [96,97]

$$\begin{aligned} T_{\rm rad}^{\rm max} = &\left(\frac{60\sqrt{3} M_p \Gamma_\phi}{g_{\rm re}\pi^2}\frac{1+\omega_\phi}{5-3\omega_\phi}\right)^{\frac{1}{4}} \\ &\times (3M_p^2 H_{\rm end}^2)^{\frac{1}{8}} \{y^{-\frac{3(1+\omega_\phi)}{5-3\omega_\phi}} - y^{-\frac{8}{5-3\omega_\phi}}\}, \end{aligned} \tag{50}$$

where $y = 8/(3+3\omega_\phi)$.

Production from inflaton and radiation bath: In this scenario, the fraction of the DM (say ξ) is produced from the inflaton through gravitational interaction with an initial momentum $p \sim m_\phi$ at the beginning of reheating, and the remaining fraction, $(1-\xi)$, is produced from the radiation bath because of a nonzero cross section $\langle\sigma v\rangle$ near the end of reheating with momentum around $p \sim 3T_{\rm re}$. Detailed study of the evolution of DM perturbation will be interesting in such a scenario which we will study later. For the present study, let us define an average momentum of the DM particles at the reheating end as

$$\begin{aligned} \langle p\rangle_{\rm re} &= \xi p_1(a_{\rm re}) + (1-\xi) p_2(a_{\rm re}), \\ \xi &= \frac{n_1(a_{\rm re})}{n_1(a_{\rm re}) + n_2(a_{\rm re})}, \end{aligned} \tag{51}$$

where $n_1(a_{\rm re})$ and $p_1(a_{\rm re})$ represent number density and momentum, respectively, for the gravitationally produced DM at reheating end, whereas $n_2(a_{\rm re})$ and $p_2(a_{\rm re})$ represent corresponding number density and momentum at the end of reheating for the particles produced from radiation bath. As described before, the DM particles produced gravitationally

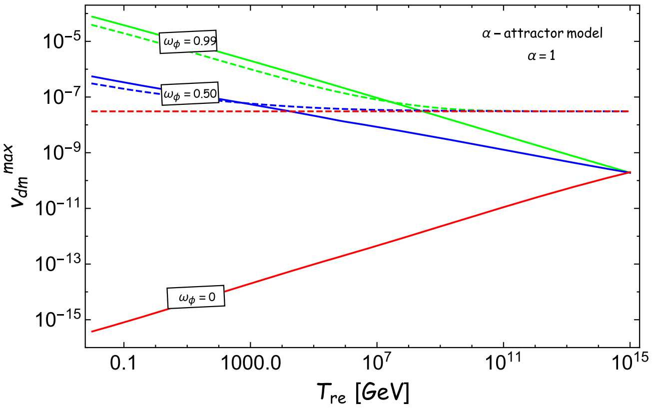

FIG. 9. We have plotted the upper bound on the present DM velocity $v_{\rm dm}^{\rm max}$ as a function of reheating temperature for three distinct values of $\omega_\phi = (0, 0.5, 0.99)$. Here, solid lines indicate results for DM production from inflaton, whereas the dashed line is for production from both the inflaton and radiation bath. In the case of production from both the inflaton and thermal bath, we choose $\xi = 0.5$. These bounds are estimated in the choice of $m_{\rm wdm} > 3.9$ keV.

from inflaton redshifts due to expansion from $a_{\rm in} = a_{\rm max}$ (corresponding to the maximum radiation temperature) till the reheating end are hence,

$$p_1(a_{\rm re}) = \frac{a_{\rm in}}{a_{\rm re}} p_{\rm in} = \left(\frac{T_{\rm re}}{T_{\rm rad}^{\rm max}}\right)^{\frac{8}{3(1+\omega_\phi)}} m_\phi. \qquad (52)$$

Upon substituting the above equation into Eq. (51), the average momentum of the DM particles at the end of the reheating is estimated as

$$\langle p\rangle_{\rm re} = \xi \left(\frac{T_{\rm re}}{T_{\rm rad}^{\rm max}}\right)^{\frac{8}{3(1+\omega_\phi)}} m_\phi + 3(1-\xi) T_{\rm re}, \qquad (53)$$

where ξ can be determined by solving Eqs. (33) and (B5). For a fixed reheating, parameters $T_{\rm re}$ and ω_ϕ to acquire a specific value of ξ with present DM abundance $\Omega_X h^2 = 0.12$, we need to choose a suitable value of the DM mass and cross section $\langle\sigma v\rangle$. Since the production rate of gravitationally produced DM is different for various types of DM, to achieve a particular value of ξ together with $\Omega_X h^2 = 0.12$, the mass of the DM must be different for a different type of DM. In Fig. 10, we have shown the DM parameter space $(m_Y, \langle\sigma v\rangle)$ for a fixed value of $\xi = 0.5$ and $\omega_\phi = (0, 0.5)$ for various types of DM. Since the momentum is redshifted by the expansion from the end of reheating till the present day, the value of the average momentum at present is

$$\langle p\rangle_{\rm now} = \frac{a_{\rm re}}{a_{\rm now}} \langle p\rangle_{\rm re} = \left(\frac{43}{11 g_s(T_{\rm re})}\right)^{1/3} \frac{T_{\rm now}}{T_{\rm re}} \langle p\rangle_{\rm re}. \qquad (54)$$

Now that we have calculated the approximate expression for the average momentum of the DM particle at the present epoch, we can put constraints on the WDM velocity depending upon the reheating equation state. Using the WDM bound, we further estimate the upper bound of the velocity of DM particles at present. The detailed constraints on the upper limit of DM velocity for two different scenarios: production from inflaton and combined production from both inflaton and radiation bath, are depicted in Fig. 9. For the case of production from inflaton, the maximum value of this upper bound turns out to be $\sim 10^{-4}$ associated with $\omega_\phi \sim 1$. From Fig. 9, we can clearly see that for $\omega_\phi = 0$, $v_{\rm dm}^{\rm max}$ for the combined case is dominated by the production from the radiation bath and turns out to be independent of reheating temperature, $v_{\rm dm}^{\rm max} \sim 3.1 \times 10^{-8}$.

A. Free streaming of DM

Understanding the free streaming behavior of the DM is important, as it plays crucial role in the process of structure formation. The larger the free streaming length, the less probable it will be to form the structure of around that

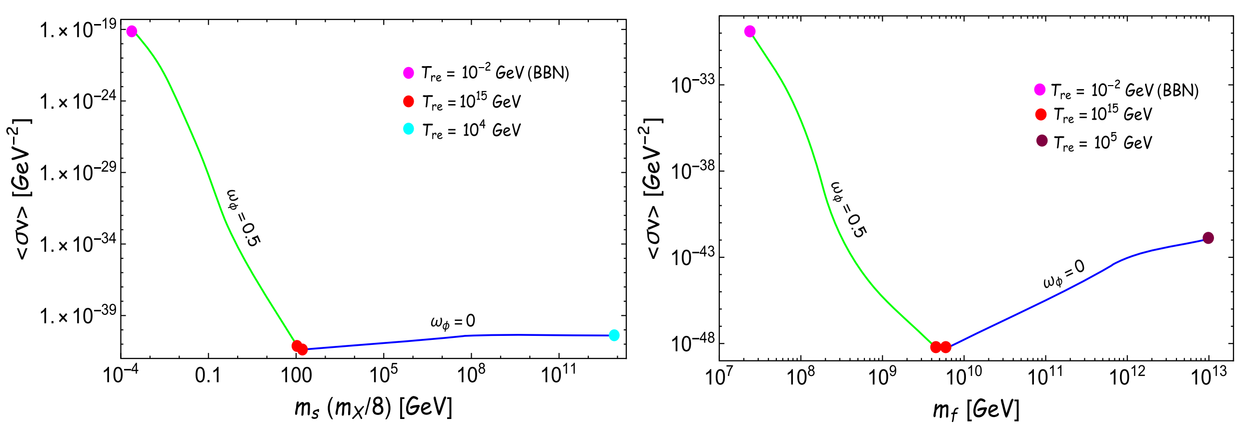

FIG. 10. $\langle\sigma v\rangle$ vs DM mass for $\xi = 0.5$ and $\omega_\phi = (0, 0.5)$. Here, for two different values of ω_ϕ, to plot DM parameters $(m_Y, \langle\sigma v\rangle)$, we vary reheating the temperature from minimum to the maximum allowed value.

length scale. If the DM particles have large initial momentum, their free-streaming effect can erase the structure on scales smaller than the free-streaming horizon $\lambda_{\rm fs}$. The free-streaming horizon strictly depends on the position where the DM particles decouple in the early Universe. In this section, we calculate the free-streaming horizon for different DM production scenarios during reheating. The free-streaming horizon is naturally related to the average momentum of the DM particles and can be approximately calculated by integrating from the time of decoupling $t_{\rm kd}$ to the present t_0 as [98–102]

$$\lambda_{\rm fs} = k_{\rm fs}^{-1} = \int_{t_{\rm kd}}^{t_0} \frac{v}{a} dt = \int_{a_{\rm kd}}^{a_0} \frac{p}{E} \frac{da}{a^2 H} = \int_{a_{\rm kd}}^{a_0} \frac{p}{\sqrt{p^2 + m_x^2}} \frac{da}{a^2 H}, \tag{55}$$

where $a_{\rm kd}$ represents scale factor associated with the decoupled time $t_{\rm kd}$. Therefore, the Hubble parameter after reheating can be related with the current Hubble rate as

$$H(a) = H_0 \sqrt{\Omega_r a^{-4} + \Omega_m a^{-3}} = a^{-2} H_0 \sqrt{\Omega_r} \sqrt{1 + a/a_{\rm eq}}, \tag{56}$$

where the scale factor at the matter-radiation equality is identified as $a_{\rm eq} = \Omega_r/\Omega_m$. We ignore dark energy contribution to the expansion. *Standard Freeze-in from thermal bath*: For comparison, we consider this scenario first. Evaluation can be divided into two regimes, the produced DM particles are relativistic after reheating ends $p_{\rm re} \gg m_Y$, and as the Universe expanses, it becomes nonrelativistic in nature $p \ll m_Y$. Therefore, the free-streaming length can be expressed as

$$k_{\rm fs}^{-1} = \int_{a_{\rm re}}^{a_{\rm nr}} \frac{da}{a^2 H} + \int_{a_{\rm nr}}^{a_0} \frac{p}{m_Y} \frac{da}{a^2 H}. \tag{57}$$

Here, $a_{\rm nr}$ indicates the scale factor at the transition between two regimes where $p_{\rm nr} = m_Y$. In the regime where DM particles are relativistic, the contribution to the free-streaming length turns out as

$$\int_{a_{\rm re}}^{a_{\rm nr}} \frac{da}{a^2 H} = \frac{1}{H_0 \sqrt{\Omega_r}} \int_{a_{\rm re}}^{a_{\rm nr}} \frac{da}{\sqrt{1 + a/a_{\rm eq}}} \simeq \frac{a_{\rm re}}{H_0 \sqrt{\Omega_r}} \left(\frac{a_{\rm nr}}{a_{\rm re}} - 1 \right) \simeq \frac{1}{k_{\rm re}} \frac{p_{\rm re}}{m_Y}. \tag{58}$$

To determine the above equation, we use the relation $a_{\rm nr}/a_{\rm re} = p_{\rm re}/p_{\rm nr} = p_{\rm re}/m_Y$, as after reheating the momentum associated with DM particles redshifts due to expansion. Further, considering $a_{\rm re} \le a \le a_{\rm nr}$, $1 + a/a_{\rm eq} \simeq 1$ $(a \ll a_{\rm eq})$, the contribution to $k_{\rm fs}^{-1}$ during the period when DM particles are nonrelativistic $(p \ll m_Y)$ becomes

$$\int_{a_{\rm nr}}^{a_0} \frac{p}{m_Y} \frac{da}{a^2 H} = \frac{p_{\rm re} a_{\rm re}}{m_Y H_0 \sqrt{\Omega_r}} \int_{a_{\rm nr}}^{1} \frac{da}{a \sqrt{1 + a/a_{\rm eq}}} = \frac{2 p_{\rm re}}{k_{\rm re} m_Y} \left[\sin h^{-1} \sqrt{\frac{a_{\rm eq}}{a_{\rm nr}}} - \sin h^{-1} \sqrt{a_{\rm eq}} \right]. \tag{59}$$

In deriving the above equation, we used the relation $k_{\rm re} a_{\rm re} = H(a_{\rm re}) a_{\rm re}^2 = H_0 \sqrt{\Omega_r}$ [derived from Eq. (56)]. Upon substituting Eqs. (58) and (59) into Eq. (57), the expression for free-streaming length becomes

$$\lambda_{\rm fs} = k_{\rm fs}^{-1} \simeq \frac{1}{k_{\rm re}} \frac{p_{\rm re}}{m_Y} \left[1 + 2 \left\{ \sin h^{-1} \sqrt{\frac{a_{\rm eq}}{a_{\rm nr}}} - \sinh^{-1} \sqrt{a_{\rm eq}} \right\} \right]. \tag{60}$$

$k_{\rm re} \sim 1/\lambda_{\rm re}$ is associated with the typical length scale that will be entering during the end of reheating. Since, our starting assumption is $p_{\rm re} \gg m_Y$, Eq. (60) indicates that $\lambda_{\rm fs}/\lambda_{\rm re} > 1$, which implies that the free-streaming effect may erases the growth of the DM perturbations produced during the reheating phase [103–105].

Interestingly, if the DM particles produced from the radiation bath is nonrelativistic $p_{\rm re} \ll m_Y$,

$$\lambda_{\rm fs} \simeq \frac{2 p_{\rm re}}{k_{\rm re} m_Y} \left[\sinh^{-1} \sqrt{\frac{a_{\rm eq}}{a_{\rm re}}} - \sinh^{-1} \sqrt{a_{\rm eq}} \right] \simeq \frac{2 \lambda_{\rm re} p_{\rm re}}{m_Y} \sinh^{-1} \sqrt{\frac{T_{\rm re}}{T_{\rm eq}}} \simeq \frac{2 p_{\rm re}}{k_{\rm re} m_x} \ln \left(2 \sqrt{\frac{T_{\rm re}}{T_{\rm eq}}} \right). \tag{61}$$

To derive the expression above, uses have been made of the relation $a_{\rm eq}/a_{\rm re} = T_{\rm re}/T_{\rm eq}$, the approximation $\sinh^{-1} x$ as $\log_e(2x)$ in the limit of $x \gg 1$ and $\sinh^{-1} \sqrt{a_{\rm eq}/a_{\rm re}} > \sinh^{-1} \sqrt{a_{\rm eq}}$. The condition for small scale structures of length scales $\lambda_{\rm re}$ being formed are if one satisfies

$$\lambda_{\rm re} > \lambda_{\rm fs} \Rightarrow \frac{T_{\rm re}}{T_{\rm eq}} < \frac{1}{4} e^{\frac{m_Y}{3 T_{\rm re}}}, \tag{62}$$

where $T_{\rm eq} \simeq 0.8$ eV at the radiation-matter equality. In addition, above the constraint can be converted into the constraint on the velocity of the DM particle during the end of reheating as $v_{\rm re} < \frac{1}{4 \ln(\frac{T_{\rm re}}{T_{\rm eq}})}$. As an example, for reheating temperatures $T_{\rm re} = (10^{-2}, 10^2, 10^6)$ GeV, the upper bound on $v_{\rm re}$ turns out as $v_{\rm re} < (6 \times 10^{-2}, 10^{-2}, 7 \times 10^{-3})$ accordingly.

Gravitational DM from inflaton: As has been discussed earlier, the gravitationally produced DM from the inflaton mostly occurred at the beginning of the reheating when the temperature is approximately taken as maximum radiation temperature, $T_{\rm in} = T_{\rm rad}^{\rm max}$. And the initial momentum of the DM particle would be the same as inflaton mass $p_{\rm in} = m_\phi$.

As the DM has no interaction with the radiation bath, the momentum of the DM particles decreases as $1/a$ after $a = a_{\rm max}$. Therefore, the free streaming will have nontrivial dependence on the reheating equation of state for this scenario. Considering DM particles are relativistic until the end end of the reheating, $\lambda_{\rm fs}$ can be expressed as

$$\lambda_{\rm fs} = k_{\rm fs}^{-1} = \int_{a_{\rm in}(a_{\rm max})}^{a_{\rm re}} \frac{da}{a^2 H} + \int_{a_{\rm re}}^{a_{\rm nr}} \frac{da}{a^2 H} + \int_{a_{\rm nr}}^{a_0} \frac{p}{m_x} \frac{da}{a^2 H}. \quad (63)$$

In the reheating regime, the contribution to the free-streaming length is given by

$$\int_{a_{\rm max}}^{a_{\rm re}} \frac{da}{a^2 H} = \frac{1}{H_{\rm re} a_{\rm re}^{\frac{3}{2}(1+\omega_\phi)}} \int_{a_{\rm max}}^{a_{\rm re}} a^{\frac{1}{2}(3\omega_\phi - 1)} da$$
$$= \frac{2}{(1+3\omega_\phi) k_{\rm re}} \left[1 - \left(\frac{a_{\rm max}}{a_{\rm re}}\right)^{\frac{1}{2}(3\omega_\phi+1)}\right], \quad (64)$$

where $H_{\rm re}$ represents Hubble parameter at the end of the reheating. To determine the above equation, we assume the variation of the Hubble parameter during reheating phase as $H(a) = H_{\rm re}(\frac{a_{\rm re}}{a})^{\frac{3}{2}(1+\omega_\phi)}$, under the assumption that the reheating phase is dominated by the inflaton equation of state ω_ϕ. In addition to that, for the perturbative reheating scenario, the scale factor at the point of maximum radiation temperature is calculated as

$$a_{\rm max} = a_{\rm end} \left(\frac{8}{5 - 3\omega_\phi}\right)^{\frac{2}{5-3\omega_\phi}}, \qquad a_{\rm end} = \frac{e^{N_k} k}{H_k}, \quad (65)$$

where the scale factor at the end of the inflation symbolizes by $a_{\rm end}$. Combining Eqs. (58), (59), (63), and (64), we obtain the expression of the free-streaming length for gravitationally produced DM as follows:

$$\lambda_{\rm fs} \simeq \frac{1}{k_{\rm re}} \left[\frac{2}{1+3\omega_\phi} \left\{1 - \left(\frac{a_{\rm max}}{a_{\rm re}}\right)^{\frac{1}{2}(3\omega_\phi+1)}\right\} + \frac{p_{\rm re}}{m_x} \left\{1 + 2\left(\sinh^{-1}\sqrt{\frac{a_{\rm eq}}{a_{\rm nr}}} - \sinh^{-1}\sqrt{a_{\rm eq}}\right)\right\}\right]. \quad (66)$$

In this scenario, when gravitationally produced DM particles are relativistic at the time of production as well as at the end of the reheating, Eq. (66) indicates that $\lambda_{\rm fs}/\lambda_{\rm re} > 1$. On the other hand, if the gravitationally produced DM particles are relativistic at the time of production but become nonrelativistic at the time of reheating end ($p_{\rm re} = m_Y$), one obtains

$$\frac{\lambda_{\rm fs}}{\lambda_{\rm re}} \simeq \frac{2}{1+3\omega_\phi} \left\{1 - \left(\frac{a_{\rm max}}{a_{\rm re}}\right)^{\frac{1}{2}(3\omega_\phi+1)}\right\} + \frac{2 p_{\rm re}}{m_x} \left(\sinh^{-1}\sqrt{\frac{a_{\rm eq}}{a_{\rm re}}} - \sinh^{-1}\sqrt{a_{\rm eq}}\right). \quad (67)$$

Since $a_{\rm max}/a_{\rm re} \ll 1$, and with the help of Eq. (61), the ratio $\lambda_{\rm fs}/\lambda_{\rm re}$ can be approximately expressed as

$$\frac{\lambda_{\rm fs}}{\lambda_{\rm re}} \simeq \frac{2}{1+3\omega_\phi} + 2 \ln\left(2\sqrt{\frac{T_{\rm re}}{T_{\rm eq}}}\right). \quad (68)$$

For $\lambda_{\rm fs} < \lambda_{\rm re}$, constraints on the reheating temperature $T_{\rm re}$ will be

$$T_{\rm re} < \frac{1}{4} T_{\rm eq} e^{\frac{3\omega_\phi - 1}{3\omega_\phi + 1}}. \quad (69)$$

From the above equation, we can clearly notice that the bound on reheating temperature turns out as $T_{\rm re} \ll 10^{-2}$ GeV, which violates the BBN constraints. Therefore, we can conclude that if the DM particles are relativistic until the reheating end, the free streaming length will be large enough to suppress the small-scale structure naturally.

Similar to the previous case, if gravitationally produced DM particles become nonrelativistic any time during the reheating,

$$\lambda_{\rm fs} = \int_{a_{\rm in}(a_{\rm max})}^{a_{\rm nr}} \frac{da}{a^2 H} + \int_{a_{\rm nr}}^{a_{\rm re}} \frac{p}{m_x} \frac{da}{a^2 H} + \int_{a_{\rm re}}^{a_0} \frac{p}{m_x} \frac{da}{a^2 H}. \quad (70)$$

The first term on the right-hand side of the above equation evaluated as

$$\int_{a_{\rm max}}^{a_{\rm nr}} \frac{da}{a^2 H} \simeq \frac{2}{(1+3\omega_\phi) k_{\rm re}} \times \left[\left(\frac{a_{\rm nr}}{a_{\rm re}}\right)^{\frac{1}{2}(3\omega_\phi+1)} - \left(\frac{a_{\rm max}}{a_{\rm re}}\right)^{\frac{1}{2}(3\omega_\phi+1)}\right], \quad (71)$$

where

$$\frac{a_{\rm nr}}{a_{\rm re}} = \frac{p_{\rm re}}{p_{\rm nr}} = \frac{p_{\rm re}}{m_x}, \qquad \frac{a_{\rm max}}{a_{\rm re}} = \frac{p_{\rm re}}{p_{\rm in}} = \frac{p_{\rm re}}{m_x} \frac{m_x}{m_\phi}. \quad (72)$$

Upon substitution of Eq. (72) into Eq. (71) and further considering $m_\phi \gg m_Y$, one finds

$$\int_{a_{\rm max}}^{a_{\rm nr}} \frac{da}{a^2 H} \simeq \frac{2}{(1+3\omega_\phi) k_{\rm re}} \left(\frac{p_{\rm re}}{m_x}\right)^{\frac{1}{2}(3\omega_\phi+1)}. \quad (73)$$

Accordingly, the second term on the right-hand side of Eq. (70) estimated as

$$\int_{a_{\rm nr}}^{a_{\rm re}} \frac{p}{m_x}\frac{da}{a^2 H} \simeq \frac{p_{\rm re} a_{\rm re}}{m_x H_{\rm re} a_{\rm re}^{\frac{3}{2}(1+\omega_\phi)}} \int_{a_{\rm nr}}^{a_{\rm re}} a^{\frac{3}{2}(\omega_\phi - 1)} da = \frac{2}{(3\omega_\phi - 1)} \frac{p_{\rm re}}{k_{\rm re} m_x}\left[1 - \left(\frac{p_{\rm re}}{m_x}\right)^{\frac{1}{2}(3\omega_\phi - 1)}\right]. \tag{74}$$

Therefore, connecting Eqs. (70), (73), (74), and (61), one can find the following expression of free-streaming length:

$$\lambda_{\rm fs} \simeq \lambda_{\rm re}\left[\frac{4}{1-9\omega_\phi^2}\left(\frac{p_{\rm re}}{m_x}\right)^{\frac{1}{2}(1+3\omega_\phi)} + \frac{p_{\rm re}}{m_x}\left\{\frac{2}{3\omega_\phi - 1} + 2\ln\left(2\sqrt{\frac{T_{\rm re}}{T_{\rm eq}}}\right)\right\}\right]. \tag{75}$$

For this case, the condition $\lambda_{\rm fs}/\lambda_{\rm re} < 1$, will lead to following constraint relation among the inflaton equation of state, DM mass, and reheating temperature:

$$\left(\frac{T_{\rm re}}{T_{\rm rad}^{\rm max}}\right)^{\frac{8}{3(1+\omega_\phi)}}\left[\frac{4}{1-9\omega_\phi^2}\left(\frac{T_{\rm re}}{T_{\rm rad}^{\rm max}}\right)^{\frac{4(3\omega_\phi - 1)}{3(1+\omega_\phi)}}\left(\frac{m_\phi}{m_x}\right)^{\frac{3\omega_\phi - 1}{2}} + \frac{2}{3\omega_\phi - 1} + 2\ln\left(2\sqrt{\frac{T_{\rm re}}{T_{\rm eq}}}\right)\right] < \frac{m_x}{m_\phi}. \tag{76}$$

The above constraint can be further transformed into constraint on the velocity of DM particles as

$$\frac{4}{1-9\omega_\phi^2} v_{\rm re}^{\frac{1+3\omega_\phi}{2}} + v_{\rm re}\left\{\frac{2}{3\omega_\phi - 1} + 2\ln\left(2\sqrt{\frac{T_{\rm re}}{T_{\rm eq}}}\right)\right\} < 1. \tag{77}$$

We now have all the necessary analytical along with the numerical results to understand the region in the parameter space of reheating temperature and DM mass and inflaton equation of state. The condition $\lambda_{\rm fs}/\lambda_{\rm re} < 1$ is expected to play important role in the formation of small-scale structures. As one would expect, the effect of free-streaming on the DM structures of length scale above the free-streaming horizon should be negligible. The numerical value of scales around which free streaming may have an effect can be estimated from Fig. 12 (shaded region) as a function of DM mass (upper panel) and reheating temperature (lower panel) for different kinds of DM particles with three distinct values of the inflaton equation of state $\omega_\phi = (0, 0.2, 0.5)$. As an example, the permitted range of scales to sustain small scale structure lies in between $\{(5\times 10^{11}, 5\times 10^{18}), (5\times 10^5, 2\times 10^{16})\}$ Mpc^{-1} for scalar DM, $\{(3\times 10^{12}, 8\times 10^{18}), (5\times 10^5, 10^{17})\}$ Mpc^{-1} for vector DM and $\{(10^{13}, 10^{19}), (5\times 10^5, 10^{19})\}$ Mpc^{-1} for fermionic DM with EoS $\omega_\phi = (0, 0.2)$ accordingly. Moreover, for $\omega_\phi = 0.5$, there is no allowed range of scales above the free-streaming horizon for scalar and vector DM, whereas for fermionic DM, the permitted range lies within $(5\times 10^5, 10^{14})$ Mpc^{-1}. We should mention at this point that the detailed effects of free-streaming can be understood from the dynamics of the DM perturbation, which we will study in the future.

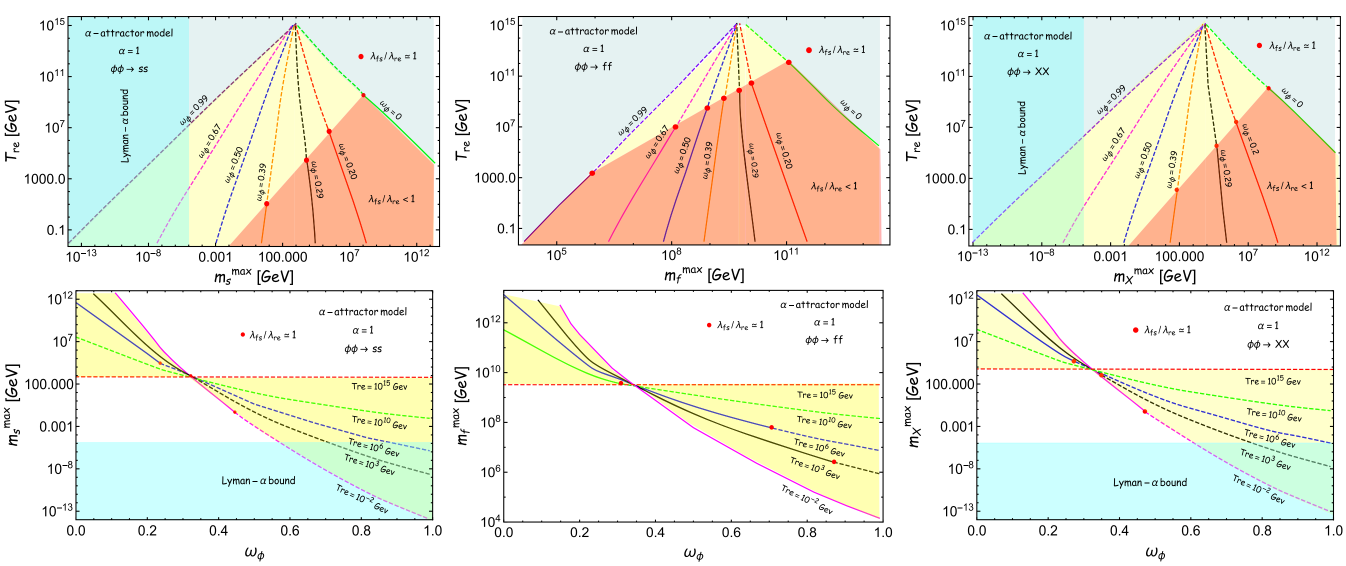

FIG. 11. Upper panel : We have shown the region (indicated by orange color) in the $T_{\rm re}$, $m_Y^{\rm max}$ plane, where the free-streaming effect does not hamper the small-scale structures formed during the reheating phase. The red circle corresponding to that point where $\lambda_{\rm fs}/\lambda_{\rm re} \simeq 1$. The other description of these figures is the same as Fig. 1. Lower panel: We have shown the parameters compatible with the condition $\lambda_{\rm fs}/\lambda_{\rm re} < 1$ through the solid line and dotted line for $\lambda_{\rm fs}/\lambda_{\rm re} > 1$ with different sets of reheating temperatures. The additional description of these last three figures is given in Fig. 2.

TABLE III. Different inflaton equation of state and reheating temperature (measured in GeV), associated bound on $v_{\rm re}$, considering purely gravitational production of DM.

	$\omega_\phi = 0$			$\omega_\phi = 0.2$			$\omega_\phi = 0.5$		
Parameter	$T_{\rm re} = 10^{-2}$	$T_{\rm re} = 10^{3}$	$T_{\rm re} = 10^{6}$	$T_{\rm re} = 10^{-2}$	$T_{\rm re} = 10^{3}$	$T_{\rm re} = 10^{6}$	$T_{\rm re} = 10^{-2}$	$T_{\rm re} = 10^{3}$	$T_{\rm re} = 10^{6}$
$v_{\rm re}^{\rm max}$	0.024	0.017	0.015	0.040	0.027	0.022	0.049	0.031	0.026

TABLE IV. Different reheating temperature (measured in units of GeV), associated limits on the inflaton equation of state and DM mass m_Y (measured in units of GeV), emerging from the free-streaming effect.

	$T_{\rm re} = 10^{-2}$			$T_{\rm re} = 10^{3}$			$T_{\rm re} = 10^{6}$		
Parameters	$\phi\phi \to SS$	$\phi\phi \to ff$	$\phi\phi \to XX$	$\phi\phi \to SS$	$\phi\phi \to ff$	$\phi\phi \to XX$	$\phi\phi \to SS$	$\phi\phi \to ff$	$\phi\phi \to XX$
$\omega_\phi^{\rm max}$	0.45	1.00	0.47	0.33	0.87	0.35	0.24	0.71	0.27
$m_Y^{\rm max}(\rm min)$	10^{-2}	1.4×10^4	2.0×10^{-2}	650	2.5×10^6	10^3	2.0×10^4	6.0×10^7	4.0×10^4

Anyway, free-streaming effects also impose constraints on the reheating and DM parameters $T_{\rm re}, \omega_\phi$, and $m_Y^{\rm max}$, shown in Fig. 11. In the upper three plots of Fig. 11, the brown shaded region corresponds to $\lambda_{\rm re} > \lambda_{\rm fs}$. Therefore, any observation of small-scale DM halos will discard the yellow shaded regions and put constraints on the upper bound on reheating temperature. For example, the upper limit on the reheating temperature will be brought down from 10^{15} GeV $\to (3.7 \times 10^9, 10^{12}, 1.0 \times 10^{10})$ GeV for $\phi\phi \to SS/ff/XX$ for inflaton EoS $\omega_\phi = 0$. Gravitational production has a one-to-one correspondence between reheating temperature and DM mass. Hence, the upper limit on reheating temperature leads to lower limit on the maximum possible DM mass $m_Y^{\rm max}$ as $(9.0 \times 10^2, 10^{10}, 7 \times 10^3)$ GeV $\to$ $(10^8, 10^{11}, 3.0 \times 10^8)$ GeV for $\phi\phi \to SS/ff/XX$, respectively. The details of the constraints on the $T_{\rm re}$ and $m_Y^{\rm max}$ for different sets of the inflaton equation of state can be read off from the Fig. 11 (first three plots). In the last three plots of Fig. 11, we observe the possible constraints on the inflaton equation of state ω_ϕ and $m_Y^{\rm max}$ due to the free-streaming effect for different sets of $T_{\rm re}$. The numerical values of the possible limitation on $\omega_\phi, m_Y^{\rm max}$ for three distinct reheating temperatures $T_{\rm re} = (10^{-2}, 10^3, 10^6)$ GeV are provided in Table IV. In addition to that, in Table III, we have shown the possible constraints on the maximum DM velocity at the end of reheating for different sets of $(T_{\rm re}, \omega_\phi)$.

At the end, we would like to point out that during the reheating phase, there is a growth in DM density perturbation due to gravitational instability. The early DM microhalos can be formed from that enhanced perturbation if the free-steaming length is smaller than the horizon. This growth in perturbation modified the DM annihilation rate by several orders [105] and strictly depended on the microhalos' formation time. Our eventual plan in the future is to study the growth of the DM perturbation in the present context.

VIII. CONCLUSIONS

In this paper, our focus is on the two main topics of DM phenomenology. In the first half, we studied the production of DM matter from the scattering of inflatons mediated by gravitons. For completeness, we also include the production from radiation bath. This is the reason in the ($\langle\sigma v\rangle$ vs m_Y) parameter space, the gravitationally produced DM appeared to have unique mass value $m_Y^{\rm max}$ (see Figs. 5, 4) for which the present DM abundance is satisfied. The value of $m_Y^{\rm max}$ is uniquely determined by the inflationary energy scale $H_{\rm end}$, and inflaton effective equation of state during reheating ω_ϕ (see Figs. 1, 2), which are expressed in Eq. (29). We studied the constraint on the DM mass considering vector, scalar, and fermion type DM considering both CMB power spectrum and the DM abundance. For bosonic DM, the observationally viable mass range turned out to be within $(10^{13}\text{–}10^{-14})$ GeV. Therefore, gravitationally produced DM of mass in the eV range can be identified as axion field. However, in order to obtain such a low bosonic DM mass through gravitational production, we found that reheating equation of state needs to be closed to unity, which is equivalent to kination domination. We will study this fact in detail in the future. For fermionic DM, the mass range turned out to be $m_f^{\rm max} = (10^{13}\text{–}10^4)$ GeV. Importantly, it is observed that allowed DM mass range shrinks to a point as ω_ϕ approaches towards $1/3$, which is clearly observed in Fig. 2. We have discussed single component and two-component DM scenarios and discussed the constraints on the DM parameters consistent with both CMB and DM abundance.

In the second half of the paper, we discussed the phase space distribution and the free streaming properties. These are the properties that are believed to capture the microscopic properties of DM. The formation of structure at all scales is crucially dependent on these intrinsic properties of the DM, which has gained interest in the recent past. The phase-space distribution has been shown to be crucially

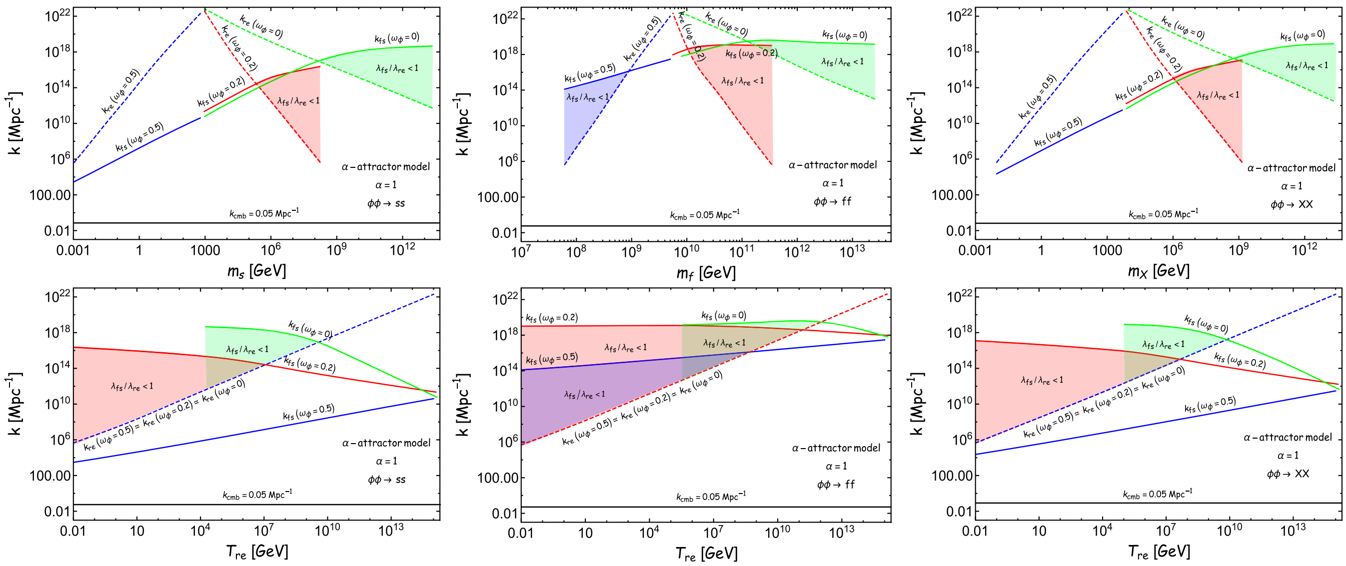

FIG. 12. We have plotted the variation of $k_{\rm fs}$ and $k_{\rm re}$ as a function of DM mass m_Y and reheating temperature $T_{\rm re}$ for three different gravitationally produced DM scenarios: $\phi\phi \to SS$ (scalar DM), $\phi\phi \to ff$ (fermionic DM), and $\phi\phi \to XX$ (vector DM) with three different inflaton equations of state $\omega_\phi = (0, 0.2, 0.5)$ (in green, red and blue). The shaded region indicates the parameter space in the $k - m_Y$ and $k - T_{\rm re}$ plane, where the free-streaming length of DM particles does not erase structures on small scales formed during reheating era.

dependent on the production mechanism and the background dynamics (see Fig. 8). The bosonic DM phase-space distribution function contains the equation of state-dependent peak at the initial moment of DM production, and the associated momentum of the particle is of the order of inflaton mass with which DM particles will subsequently start to free stream. Interestingly the fermionic phase-space distribution function contains an additional peak in the later time, which arises due to the fermionic annihilation rate $\Gamma_{\phi\phi\to ff}$ nontrivially depending upon the decaying inflaton mass. This secondary peak height is naturally dependent upon the reheating temperature; as the reheating temperature reduces, the peak height increases, which can be observed in Fig. 8. Considering free streaming horizon, we have divided the allowed range of DM mass in terms of $T_{\rm re}$ and ω_ϕ (see Fig. 11) into two subranges for $\lambda_{\rm re} > \lambda_{\rm fs}$ depicted by the brown shaded region in the upper panel and solid lines in the lower panel and for $\lambda_{\rm re} < \lambda_{\rm fs}$ depicted by the yellow shaded region in the upper panel and dotted lines in the lower panel. Finally, in Fig. 12, we plotted allowed ranges of scales associated with the free-streaming horizon around which small DM halos can be formed. Shaded regions correspond to $\lambda_{\rm fs} < \lambda_{\rm re}$, which indicate that due to gravitational pull, small scale DM halos can be formed associated with those scales during reheating. If those small-scale structures are detected, DM matter mass parameter space, inflaton equation of state, and reheating temperature will be significantly constrained.

ACKNOWLEDGMENTS

M. R. H would like to thank the Ministry of Human Resource Development, Government of India (GoI), for financial assistance. D. M wish to acknowledge support from the Science and Engineering Research Board (SERB), Department of Science and Technology (DST), GoI, through the Core Research Grant No. CRG/2020/003664. We like to thank the HEP and Gravity groups at IIT Guwahati for useful discussions.

APPENDIX A: ANALYTIC EXPRESSION OF MAXIMUM DM MASS $m_Y^{\rm max}$

The expression for the relic abundance Eq. (27) indicates that the DM abundance increases with increasing the DM mass. Consequently, there should exist a maximum allowed DM mass $m_Y^{\rm max}$ associated with each viable value of the spectral index or reheating temperature. The evolution of the gravitationally produce DM number density follows form the equation,

$$d(n_Y a^3) = \frac{\Gamma_{\phi\phi\to YY}}{m_\phi} \frac{\rho_\phi(1+\omega_\phi)}{H} a^2 da. \qquad \text{(A1)}$$

Comoving number density of scalar DM: The comoving number density at the end of the reheating era is followed by the Eqs. (2), (A1) and found to be

$$n_s^{\rm re} A_{\rm re}^3 = \int_1^{A_{\rm re}} \frac{\rho_\phi^2(1+\omega_\phi)}{1024\pi M_p^4}\left(1+\frac{m_s^2}{2m_\phi^2}\right)\sqrt{1-\frac{m_s^2}{m_\phi^2}}\frac{A^2 dA}{H}$$
$$\approx \int_1^{A_{\rm re}} \frac{\rho_\phi^2(1+\omega_\phi)}{1024\pi M_p^4}\frac{A^2 dA}{H}. \qquad \text{(A2)}$$

Ignoring the subdominated effect of the DM production into the evolution of the inflaton energy density, the inflaton energy density shall follow the following equation:

$$\rho_\phi = \rho_\phi^{\rm end} A^{-3(1+\omega_\phi)} e^{-\Gamma_\phi(1+\omega_\phi)(t-t_{\rm end})} \approx \rho_\phi^{\rm end} A^{-3(1+\omega_\phi)}, \quad (A3)$$

where $\rho_\phi^{\rm end}$ is the inflaton energy density at the end of the inflation. As the initial stage of the perturbative reheating is dominated by the inflaton energy density, the main contribution in the gravitationally produced DM sector is coming at the initial stage. Therefore, we can ignore the effect of the decay constant Γ_ϕ in determining the gravitationally produced DM number density. The Hubble parameter during perturbative reheating can be approximated as

$$H = H_{\rm end} A^{-\frac{3}{2}(1+\omega_\phi)}, \quad (A4)$$

where $H_{\rm end} = \sqrt{\rho_\phi^{\rm end}/3M_p^2}$ is the Hubble parameter at the end of the inflation. Upon substituting the Eqs. (A3) and (A4) in the expression of the comoving gravitationally produced DM number density [Eqs. (A2)], we obtain

$$n_s^{\rm re} A_{\rm re}^3 \approx \frac{(\rho_\phi^{\rm end})^2(1+\omega_\phi)}{1024\pi M_p^4 H_{\rm end}} \int_1^{Are} A^{-\frac{1}{2}(5+3\omega_\phi)} dA = \frac{3}{512\pi} \frac{(1+\omega_\phi)}{(1+3\omega_\phi)} H_{\rm end}^3 [1 - A_{\rm re}^{-\frac{3}{2}(1+3\omega_\phi)}]. \quad (A5)$$

Comoving number density of fermionic DM: The relic abundance of the DM is obtained from the comoving DM number density, calculated at the end of the reheating. Inserting the expression for the annihilation rate Eq. (4) into the Eq. (A1), the corresponding number density of the DM for this present scenario turns out to be

$$n_f^{\rm re} A_{\rm re}^3 = \int_1^{A_{\rm re}} \frac{\rho_\phi^2 m_f^2 (1+\omega_\phi)}{4096\pi M_p^4 m_\phi^2} \left(1 - \frac{m_f^2}{m_\phi^2}\right) \frac{A^2 dA}{H} \approx \int_1^{A_{\rm re}} \frac{\rho_\phi^2 m_f^2 (1+\omega_\phi)}{4096\pi M_p^4 m_\phi^2} \frac{A^2 dA}{H}. \quad (A6)$$

The inflaton mass m_ϕ^2 can be calculated from the second derivative of the inflaton potential. Since reheating happens near the minimum of the potential, we first expand the inflaton potential in the limit of $\phi \ll M_p$ as

$$V(\phi) \simeq \lambda \phi^{2n}, \quad (A7)$$

where $\lambda = \Lambda^4 (\sqrt{\frac{2}{3\alpha}} \frac{1}{M_p})^{2n}$. Therefore,

$$m_\phi^2 = V''(\phi_0(t)) \simeq 2n(2n-1) \lambda^{\frac{1}{n}} \rho_\phi^{\frac{n-1}{n}}. \quad (A8)$$

Upon substituting the Eqs. (A8), (A4), and (A3) into the expression (A6), one can find the gravitationally produced comoving fermionic DM number density at the end of reheating as

$$n_f^{\rm re} A_{\rm re}^3 = \frac{H_{\rm end}^3 m_f^2 \lambda^{\frac{\omega_\phi - 1}{\omega_\phi + 1}} \nu(\omega_\phi)}{4096\pi(1+3\omega_\phi)(H_{\rm end}^2 M_p^2)^{\frac{2\omega_\phi}{1+\omega_\phi}}} [1 - A_{\rm re}^{-\frac{3}{2}(1-\omega_\phi)}] \simeq \frac{3}{2048\pi} \frac{1+\omega_\phi}{1-\omega_\phi} H_{\rm end}^3 \left(\frac{m_f}{m_\phi^{\rm end}}\right)^2, \quad (A9)$$

where $\nu(\omega_\phi) = 3^{\frac{1-\omega_\phi}{1+\omega_\phi}}(1-\omega_\phi)$ and $m_\phi^{\rm end}$ indicates effective mass calculated at the end of the inflation. We use the relation $\omega_\phi = (n-1)/(n+1)$ to find the above relation of comoving DM number density in terms of ω_ϕ.

Comoving number density of vector DM: For vector DM, the comoving number density can be written as [combining Eqs. (4) and (A1)]

$$n_X^{\rm re} A_{\rm re}^3 = \int_1^{A_{\rm re}} \frac{\rho_\phi^2 (1+\omega_\phi)}{32768\pi M_p^4} \sqrt{1 - \frac{m_X^2}{m_\phi^2}} \left(4 + 4\frac{m_X^2}{m_\phi^2} + 19\frac{m_X^4}{m_\phi^4}\right) \times \frac{A^2 dA}{H} \approx \int_1^{A_{\rm re}} \frac{\rho_\phi^2 (1+\omega_\phi)}{8192\pi M_p^4} \frac{A^2 dA}{H}. \quad (A10)$$

We can see that in the limit of $m_X \ll m_\phi$, the above expression can be related with the comoving number density for the scalar DM [Eq. (A2)] through a $1/8$ factor. Therefore,

$$n_X^{\rm re} A_{\rm re}^3 = \frac{1}{8} n_s^{\rm re} A_{\rm re}^3 = -\frac{3}{4096\pi} \frac{(1+\omega_\phi)}{(1+3\omega_\phi)} H_{\rm end}^3 [A_{\rm re}^{-\frac{3}{2}(1+3\omega_\phi)} - 1]. \quad (A11)$$

Expression for $m_Y^{\rm max}$: As we mentioned earlier, the DM relic $\Omega_Y h^2$ could be expressed in terms of present radiation abundance $\Omega_R h^2$ as

$$\Omega_Y h^2 = \frac{\rho_Y(A_{\rm re})}{\rho_R(A_{\rm re})} \frac{T_{\rm re}}{T_{\rm now}} \Omega_r h^2 = \frac{m_Y A_{\rm re}^{-3} (n_Y^{\rm re} A_{\rm re}^3)}{\beta T_{\rm re}^3 T_{\rm now}} \Omega_r h^2, \quad (A12)$$

where $\beta = \pi^2 g_{\rm re}/30$. In the context of the perturbative reheating dynamics, one can obtain the approximate analytical expression for the reheating temperature $T_{\rm re}$ and the normalized scale factor $A_{\rm re}$ at the end of the reheating to be (in this context, see Ref. [96])

$$T_{\rm re} = \mathcal{G} Are^{-1}, \qquad \mathcal{G} = \left(\frac{43}{11 g_{s,re}}\right)^{\frac{1}{3}} \left(\frac{a_0 T_0}{k}\right) H_k e^{-N_k},$$
$$A_{\rm re} = \left(\frac{12 M_p^2 H_{\rm end}^2 (1+\omega_\phi)^2}{\mathcal{G}^4 \beta (5 - 3\omega_\phi)^2}\right)^{\frac{-1}{(1-3\omega_\phi)}}. \quad (A13)$$

Inserting the expression of the reheating temperature into the expression of the present-day DM relic (admitting only gravitationally produced DM), the maximum allowed DM mass can be written as

$$m_Y^{\max} = \frac{\mathcal{G}\beta T_{\rm now}}{n_Y^{\rm re} A_{\rm re}^3} \frac{\Omega_Y h^2}{\Omega_r h^2}. \tag{A14}$$

By utilizing the above equations with the expression of the comoving number density for gravitationally produced DM [Eqs. (A5), (A9), and (A11)], we can easily fix $m_Y^{\max}$.

APPENDIX B: AN ANALYTICAL EXPRESSION FOR THE DM NUMBER DENSITY: PRODUCED FROM RADIATION BATH

The relevant Boltzmann equation for the DM particles produced from the radiation bath during perturbative reheating can be expressed as

$$\begin{aligned} d(n_x a^3) &= -a^3\langle\sigma v\rangle[n_x^2 - (n_x^{\rm eq})^2]dt \\ &= -a^2\langle\sigma v\rangle[n_x^2 - (n_x^{\rm eq})^2]\frac{dt}{H}. \end{aligned} \tag{B1}$$

Let us assume that the DM particles are relativistic ($m_x \ll T$) and never reach chemical equilibrium ($n_x \ll n_x^{\rm eq}$) during reheating. Therefore Eq. (B1) can be approximated as

$$d(n_x a^3) = \frac{a^3\langle\sigma v\rangle(n_x^{\rm eq})^2}{aH} da \simeq \frac{g^2}{\pi^4}\frac{a^2\langle\sigma v\rangle T^6}{H} da, \tag{B2}$$

where we use equilibrium distribution of the DM in the relativistic limit,

$$n_x^{\rm eq} = \frac{gT^3}{\pi^2}. \tag{B3}$$

Here, g counts the number of degrees of freedom associated with the DM particles. In the perturbative reheating scenario, the analytical expression for the radiation temperature during reheating can be obtained as

$$T = \gamma_3^{1/4} A^{-\frac{3}{2}(1+\omega_\phi)}, \quad \gamma_3 = \frac{6}{5-3\omega_\phi}\frac{M_p^2 H_{\rm end}}{\beta}\Gamma_\phi(1+\omega_\phi). \tag{B4}$$

Connecting Eqs. (B2), (B4), and (A4), the comoving DM number density is found to be

$$\begin{aligned} n_x A_{\rm re}^3 &= \frac{g^2}{\pi^4}\frac{\gamma_3^{3/2}\langle\sigma v\rangle}{H_{\rm end}}\int_1^{A_{\rm re}} A^{\frac{1}{4}(5-3\omega_\phi)} dA \\ &= \gamma_4\langle\sigma v\rangle(A^{\frac{3}{4}(3-\omega_\phi)} - 1), \end{aligned} \tag{B5}$$

where $\gamma_4 = \frac{4}{3(3-\omega_\phi)}\frac{g^2}{\pi^4}\frac{\gamma_3^{3/2}}{H_{\rm end}}$.

APPENDIX C: COMOVING NUMBER DENSITY OF THE GRAVITATIONALLY PRODUCED DM FROM SM SCATTERING

The evolution of the gravitational produced DM number density from the radiation bath is followed by the Eq. (32) as

$$d(n_{Y(R)}A^3) = \gamma\frac{T^8}{M_p^4}\frac{A^2 dA}{H}. \tag{C1}$$

In the perturbative reheating scenario, the analytical expression for the radiation temperature during reheating can be obtained as

$$T = \gamma_3^{1/4} A^{-\frac{3}{8}(1+\omega_\phi)}, \quad \gamma_3 = \frac{6}{5-3\omega_\phi}\frac{M_p^2 H_{\rm end}}{\beta}\Gamma_\phi(1+\omega_\phi). \tag{C2}$$

Upon substitution of the Eq. (C2) along with Eq. (A4) in Eq. (C1), the comoving number density turns out to be

$$\begin{aligned} n_{Y(R)}^{\rm re} A_{\rm re}^3 &= \frac{\gamma\gamma_3^2}{M_p^4 H_{\rm end}}\int_1^{A_{\rm re}} A^{\frac{1}{2}(1-3\omega_\phi)} dA \\ &= \frac{2}{3(1-\omega_\phi)}\frac{\gamma\gamma_3^2}{M_p^4 H_{\rm end}}[A_{\rm re}^{\frac{3}{2}(1-\omega_\phi)} - 1]. \end{aligned} \tag{C3}$$

As the normalized scale factor at the end of the reheating $A_{\rm re} \gg 1$ (except for the temperature associated with the instantaneous reheating), the above equation simplified as

$$\begin{aligned} n_{Y(R)}^{\rm re} A_{\rm re}^3 &= \frac{2}{3(1-\omega_\phi)}\frac{\gamma\gamma_3^2}{M_p^4 H_{\rm end}} A_{\rm re}^{\frac{3}{2}(1-\omega_\phi)} \\ &\simeq \frac{2\gamma}{3(1-\omega_\phi)}\frac{e^{\frac{3}{2}N_{\rm re}(3+\omega_\phi)} T_{\rm re}^8}{M_p^4 H_{\rm end}}. \end{aligned} \tag{C4}$$

To find the above-simplified form, we use the approximate analytic expression for reheating temperature $T_{\rm re} = \gamma_3^{1/4} A_{\rm re}^{-\frac{3}{8}(1+\omega_\phi)}$ [96,97].

[1] Y. Akrami *et al.* (Planck Collaboration), Astron. Astrophys. **641**, A10 (2020).
[2] É. Aubourg, S. Bailey, J. E. Bautista, F. Beutler, V. Bhardwaj, D. Bizyaev, M. Blanton, M. Blomqvist, A. S. Bolton, J. Bovy *et al.*, Phys. Rev. D **92**, 123516 (2015).
[3] D. Baumann and H. V. Peiris, Adv. Sci. Lett. **2**, 105 (2009).
[4] J. A. Vázquez, L. E. Padilla, and T. Matos, Rev. Mex. Fis. E **17**, 1 (2020).
[5] M. Kawasaki, K. Kohri, and N. Sugiyama, Phys. Rev. D **62**, 023506 (2000).
[6] G. Steigman, Annu. Rev. Nucl. Part. Sci. **57**, 463 (2007).
[7] B. D. Fields, P. Molaro, and S. Sarkar, Chin. Phys. C **38**, 339 (2014).
[8] M. Kawasaki, K. Kohri, and N. Sugiyama, Phys. Rev. Lett. **82**, 4168 (1999).
[9] K. N. Abazajian *et al.* (CMB-S4 Collaboration), arXiv:1610.02743.
[10] Y. Sofue and V. Rubin, Annu. Rev. Astron. Astrophys. **39**, 137 (2001).
[11] V. Sahni, Lect. Notes Phys. **653**, 141 (2004).
[12] R. Catena and P. Ullio, J. Cosmol. Astropart. Phys. 08 (2010) 004.
[13] Q. Guo, S. White, C. Li, and M. Boylan-Kolchin, Mon. Not. R. Astron. Soc. **404**, 1111 (2010).
[14] N. Arkani-Hamed, D. P. Finkbeiner, T. R. Slatyer, and N. Weiner, Phys. Rev. D **79**, 015014 (2009).
[15] J. L. Feng, Annu. Rev. Astron. Astrophys. **48**, 495 (2010).
[16] M. Pospelov, A. Ritz, and M. B. Voloshin, Phys. Lett. B **662**, 53 (2008).
[17] T. Tenkanen, J. High Energy Phys. 09 (2016) 049.
[18] M. Heikinheimo, T. Tenkanen, K. Tuominen, and V. Vaskonen, Proc. Sci., ICHEP2016 (**2016**) 825.
[19] L. J. Hall, K. Jedamzik, J. March-Russell, and S. M. West, J. High Energy Phys. 03 (2010) 080.
[20] X. Chu, Y. Mambrini, J. Quevillon, and B. Zaldivar, J. Cosmol. Astropart. Phys. 01 (2014) 034.
[21] M. Blennow, E. Fernandez-Martinez, and B. Zaldivar, J. Cosmol. Astropart. Phys. 01 (2014) 003.
[22] F. Elahi, C. Kolda, and J. Unwin, J. High Energy Phys. 03 (2015) 048.
[23] Y. Mambrini, N. Nagata, K. A. Olive, J. Quevillon, and J. Zheng, Phys. Rev. D **91**, 095010 (2015).
[24] N. Nagata, K. A. Olive, and J. Zheng, J. High Energy Phys. 10 (2015) 193.
[25] S. L. Chen and Z. Kang, J. Cosmol. Astropart. Phys. 05 (2018) 036.
[26] N. Bernal, M. Dutra, Y. Mambrini, K. Olive, M. Peloso, and M. Pierre, Phys. Rev. D **97**, 115020 (2018).
[27] Y. Hochberg, E. Kuflik, T. Volansky, and J. G. Wacker, Phys. Rev. Lett. **113**, 171301 (2014).
[28] Y. Hochberg, E. Kuflik, H. Murayama, T. Volansky, and J. G. Wacker, Phys. Rev. Lett. **115**, 021301 (2015).
[29] Y. Hochberg, E. Kuflik, and H. Murayama, J. High Energy Phys. 05 (2016) 090.
[30] N. Bernal and X. Chu, J. Cosmol. Astropart. Phys. 01 (2016) 006.
[31] N. Bernal, C. Cosme, and T. Tenkanen, Eur. Phys. J. C **79**, 99 (2019).
[32] M. A. G. Garcia, K. Kaneta, Y. Mambrini, and K. A. Olive, Phys. Rev. D **101**, 123507 (2020).
[33] M. A. G. Garcia, Y. Mambrini, K. A. Olive, and S. Verner, J. Cosmol. Astropart. Phys. 10 (2021) 061.
[34] A. Falkowski, J. T. Ruderman, and T. Volansky, J. High Energy Phys. 05 (2011) 106.
[35] L. Lopez Honorez and C. E. Yaguna, J. High Energy Phys. 09 (2010) 046.
[36] E. Aprile *et al.* (XENON100 Collaboration), Phys. Rev. Lett. **109**, 181301 (2012).
[37] E. Aprile *et al.* (XENON Collaboration), Phys. Rev. Lett. **121**, 111302 (2018).
[38] A. Tan *et al.* (PandaX-II Collaboration), Phys. Rev. Lett. **117**, 121303 (2016).
[39] D. S. Akerib *et al.* (LUX Collaboration), Phys. Rev. Lett. **118**, 021303 (2017).
[40] L. Anderson *et al.* (BOSS Collaboration), Mon. Not. R. Astron. Soc. **441**, 24 (2014).
[41] S. Capozziello, S. Nojiri, S. D. Odintsov, and A. Troisi, Phys. Lett. B **639**, 135 (2006).
[42] S. Capozziello and M. De Laurentis, Phys. Rep. **509**, 167 (2011).
[43] C. G. Boehmer, T. Harko, and F. S. N. Lobo, Astropart. Phys. **29**, 386 (2008).
[44] S. Nojiri, S. D. Odintsov, and V. K. Oikonomou, Phys. Rep. **692**, 1 (2017).
[45] J. F. Donoghue, Phys. Rev. D **50**, 3874 (1994).
[46] S. Y. Choi, J. S. Shim, and H. S. Song, Phys. Rev. D **51**, 2751 (1995).
[47] B. R. Holstein, Am. J. Phys. **74**, 1002 (2006).
[48] Y. Mambrini and K. A. Olive, Phys. Rev. D **103**, 115009 (2021).
[49] N. Bernal and C. S. Fong, J. Cosmol. Astropart. Phys. 06 (2021) 028.
[50] B. Barman and N. Bernal, J. Cosmol. Astropart. Phys. 06 (2021) 011.
[51] Y. Ema, R. Jinno, K. Mukaida, and K. Nakayama, J. Cosmol. Astropart. Phys. 05 (2015) 038.
[52] Y. Ema, R. Jinno, K. Mukaida, and K. Nakayama, Phys. Rev. D **94**, 063517 (2016).
[53] Y. Ema, K. Nakayama, and Y. Tang, J. High Energy Phys. 09 (2018) 135.
[54] M. Garny, M. Sandora, and M. S. Sloth, Phys. Rev. Lett. **116**, 101302 (2016).
[55] M. Garny, A. Palessandro, M. Sandora, and M. S. Sloth, J. Cosmol. Astropart. Phys. 02 (2018) 027.
[56] Y. Tang and Y. L. Wu, Phys. Lett. B **774**, 676 (2017).
[57] A. Lazar, J. S. Bullock, M. Boylan-Kolchin, R. Feldmann, O. Çatmabacak, and L. Moustakas, Mon. Not. R. Astron. Soc. **502**, 6064 (2021).
[58] S. Alam *et al.* (BOSS Collaboration), Mon. Not. R. Astron. Soc. **470**, 2617 (2017).
[59] P. Bode, J. P. Ostriker, and N. Turok, Astrophys. J. **556**, 93 (2001).
[60] M. Viel, G. D. Becker, J. S. Bolton, and M. G. Haehnelt, Phys. Rev. D **88**, 043502 (2013).
[61] V. K. Narayanan, D. N. Spergel, R. Dave, and C. P. Ma, Astrophys. J. Lett. **543**, L103 (2000).
[62] M. Viel, J. Lesgourgues, M. G. Haehnelt, S. Matarrese, and A. Riotto, Phys. Rev. D **71**, 063534 (2005).
[63] J. Baur, N. Palanque-Delabrouille, C. Yèche, C. Magneville, and M. Viel, J. Cosmol. Astropart. Phys. 08 (2016) 012.

[64] V. Iršič, M. Viel, M. G. Haehnelt, J. S. Bolton, S. Cristiani, G. Cupani, T. S. Kim, V. D'Odorico, S. López, S. Ellison *et al.*, Phys. Rev. D **96**, 023522 (2017).
[65] N. Palanque-Delabrouille, C. Yèche, N. Schöneberg, J. Lesgourgues, M. Walther, S. Chabanier, and E. Armengaud, J. Cosmol. Astropart. Phys. 04 (2020) 038.
[66] A. Garzilli, O. Ruchayskiy, A. Magalich, and A. Boyarsky, Mon. Not. R. Astron. Soc. **502**, 2356 (2021).
[67] G. Ballesteros, M. A. G. Garcia, and M. Pierre, J. Cosmol. Astropart. Phys. 03 (2021) 101.
[68] G. F. Giudice, E. W. Kolb, and A. Riotto, Phys. Rev. D **64**, 023508 (2001).
[69] D. J. H. Chung, E. W. Kolb, and A. Riotto, Phys. Rev. D **60**, 063504 (1999).
[70] D. Maity and P. Saha, Phys. Rev. D **98**, 103525 (2018).
[71] R. Kallosh and A. Linde, J. Cosmol. Astropart. Phys. 07 (2013) 002.
[72] R. Kallosh, A. Linde, and D. Roest, J. High Energy Phys. 11 (2013) 198.
[73] P. A. R. Ade *et al.* (Planck Collaboration), Astron. Astrophys. **594**, A20 (2016).
[74] F. L. Bezrukov and M. Shaposhnikov, Phys. Lett. B **659**, 703 (2008).
[75] A. A. Starobinsky, Phys. Lett. **91B**, 99 (1980).
[76] J. Ellis, M. A. G. Garcia, D. V. Nanopoulos, K. A. Olive, and S. Verner, Phys. Rev. D **105**, 043504 (2022).
[77] P. A. R. Ade *et al.* (BICEP and Keck Collaboration), Phys. Rev. Lett. **127**, 151301 (2021).
[78] M. Drewes, J. U. Kang, and U. R. Mun, J. High Energy Phys. 11 (2017) 072.
[79] Y. Shtanov, J. H. Traschen, and R. H. Brandenberger, Phys. Rev. D **51**, 5438 (1995).
[80] V. Mukhanov, *Physical Foundations of Cosmology* (Cambridge University Press, Oxford, 2005).
[81] N. Aghanim *et al.* (Planck Collaboration), Astron. Astrophys. **641**, A6 (2020); **652**, C4(E) (2021).
[82] N. Jarosik *et al.* (WMAP Collaboration), Astrophys. J. Suppl. Ser. **192**, 14 (2011).
[83] P. Hut, Phys. Lett. **69B**, 85 (1977).
[84] B. W. Lee and S. Weinberg, Phys. Rev. Lett. **39**, 165 (1977).
[85] M. I. Vysotsky, A. D. Dolgov, and Ya. B. Zeldovich, JETP Lett. **26**, 188 (1977).
[86] M. Srednicki, R. Watkins, and K. A. Olive, Nucl. Phys. **B310**, 693 (1988).
[87] P. Gondolo and G. Gelmini, Nucl. Phys. **B360**, 145 (1991).
[88] K. Griest and D. Seckel, Phys. Rev. D **43**, 3191 (1991).
[89] G. Arcadi, M. Dutra, P. Ghosh, M. Lindner, Y. Mambrini, M. Pierre, S. Profumo, and F. S. Queiroz, Eur. Phys. J. C **78**, 203 (2018).
[90] Y. Hochberg, E. Kuflik, R. Mcgehee, H. Murayama, and K. Schutz, Phys. Rev. D **98**, 115031 (2018).
[91] N. Bernal, J. Rubio, and H. Veermäe, J. Cosmol. Astropart. Phys. 10 (2020) 021.
[92] M. R. Haque, D. Maity, T. Paul, and L. Sriramkumar, Phys. Rev. D **104**, 063513 (2021).
[93] S. S. Mishra, V. Sahni, and A. A. Starobinsky, J. Cosmol. Astropart. Phys. 05 (2021) 075.
[94] F. D'Eramo and A. Lenoci, J. Cosmol. Astropart. Phys. 10 (2021) 045.
[95] S. Hoof, A. Geringer-Sameth, and R. Trotta, J. Cosmol. Astropart. Phys. 02 (2020) 012.
[96] M. R. Haque, D. Maity, and P. Saha, Phys. Rev. D **102**, 083534 (2020).
[97] D. Maity and P. Saha, Phys. Dark Universe **25**, 100317 (2019).
[98] E. Bertschinger, Phys. Rev. D **74**, 063509 (2006).
[99] A. M. Green, S. Hofmann, and D. J. Schwarz, Mon. Not. R. Astron. Soc. **353**, L23 (2004).
[100] A. M. Green, S. Hofmann, and D. J. Schwarz, J. Cosmol. Astropart. Phys. 08 (2005) 003.
[101] A. Boyarsky, J. Lesgourgues, O. Ruchayskiy, and M. Viel, J. Cosmol. Astropart. Phys. 05 (2009) 012.
[102] A. Loeb and M. Zaldarriaga, Phys. Rev. D **71**, 103520 (2005).
[103] A. L. Erickcek and K. Sigurdson, Phys. Rev. D **84**, 083503 (2011).
[104] J. Fan, O. Özsoy, and S. Watson, Phys. Rev. D **90**, 043536 (2014).
[105] A. L. Erickcek, Phys. Rev. D **92**, 103505 (2015).